

*extra*

NBSIR 75-725 (R)

# Report No. 8

## Ambient- and Elevated-Temperature Mechanical Properties of AAR M128-69-B Steel Plate Samples Taken From Fire Tested Insulated Tank Car RAX 202

---

J. G. Early

Mechanical Properties  
Metallurgy Division  
Institute for Materials  
National Bureau of Standards  
Washington, D. C.

Early, J. G., Mechanical properties of AAR  
M128-69-B steel plate samples taken from  
insulated fire tested tank car RAX 202, DOT  
Report No. FRA-OR&D/76-74, 57 pages (Available  
as PB/255-907 from the National Technical  
Information Service, Springfield, VA, 22161,  
June 1976).

*NBSIR 75-725*

May 1975

Final Report

312

*16718*

Prepared for  
**Federal Railroad Administration**  
Department of Transportation  
Washington, D. C. 20591



NBSIR 75-725

**REPORT NO. 8**  
**AMBIENT- AND ELEVATED-TEMPERATURE**  
**MECHANICAL PROPERTIES OF AAR M128-69-B**  
**STEEL PLATE SAMPLES TAKEN FROM FIRE TESTED**  
**INSULATED TANK CAR RAX 202**

---

J. G. Early

Mechanical Properties Section  
Metallurgy Division  
Institute for Materials Research  
National Bureau of Standards  
Washington, D. C. 20234

May 1975

Final Report

"This document has been prepared for the use of the Federal Railroad Administration, Department of Transportation. Responsibility for its further use rests with that agency. NBS requests that if release to the general public is contemplated, such action be taken only after consultation with the Office of Public Affairs at the National Bureau of Standards."

Prepared for  
Federal Railroad Administration  
Department of Transportation  
Washington, D. C. 20591



---

**U.S. DEPARTMENT OF COMMERCE, Rogers C.B. Morton, Secretary**  
**NATIONAL BUREAU OF STANDARDS, Ernest Ambler, Acting Director**



## TABLE OF CONTENTS

	<u>Page</u>
ABSTRACT	
1. INTRODUCTION.....	1
2. PURPOSE.....	2
3. EXPERIMENTAL PROCEDURES.....	2
3.1 Ambient-Temperature Tests.....	3
3.2 Elevated-Temperature Tests.....	3
3.2.1 Resistance Heated Tube Furnace Test Procedures.....	3
3.2.2 Internal-Resistance-Heating Test Procedures.....	4
3.2.3 Hot-Tensile Tests.....	4
3.2.4 Stress-Rupture Tests.....	5
3.3 Macroscopic and Metallographic Observations.....	5
4. RESULTS AND DISCUSSION.....	5
4.1 Ambient-Temperature Tensile Properties.....	5
4.1.1 Strain Ageing Effects.....	6
4.2 Hot-Tensile Properties.....	7
4.2.1 Comparison of Hot-Tensile Data for AAR M128 Steel.....	9
4.3 Stress-Rupture Properties.....	11
4.3.1 Comparison of Stress-Rupture Data for Tank Car Steels.....	11
4.4 Macroscopic and Metallographic Analyses.....	13
4.5 General Discussion.....	14
4.5.1 Ambient-Temperature Properties.....	15
4.5.2 Hot-Tensile Properties.....	15

TABLE OF CONTENTS (continued)

	<u>Page</u>
4.5.3 Stress-Rupture Properties.....	17
4.5.4 Metallographic Analysis.....	19
5. SUMMARY.....	20
6. CONCLUSIONS.....	22
7. ACKNOWLEDGEMENT.....	22
REFERENCES.....	24

TABLES

- I. Ambient-Temperature Tensile Properties of Specimens Taken From Car RAX 202
- II. Hot-Tensile Properties of Specimens Taken From Plate Sample TC2-(11B)
- III. Stress-Rupture Properties of Specimens Taken From Tank Car RAX 202

FIGURES

1. Schematic Diagram Showing the location of NBS Samples in Tank Car RAX 202 as Viewed from the Outside of the Tank Car.
2. Plate Sample TC2-(1), Shell Course 3.
3. Plate Sample TC2-(3), Shell Course 3.
4. Plate Sample TC2-(11), Shell Course 1 and Shell Course 2.
5. Elevated-Temperature Strength Properties of Plate Sample TC2-(11B), AAR M128-B Steel, Taken from Tank Car RAX 202.
6. Elevated-Temperature Tensile Ductility Properties of Plate Sample TC2-(11B), AAR M128-B Steel, Taken from Tank Car RAX 202.
7. Elevated-Temperature Ultimate Tensile Strength Properties of AAR M128-B Steel.
8. Elevated-Temperature Yield Strength Properties of AAR M128-B Steel.
9. Stress-Rupture Data for Three Plate Samples from Tank Car RAX 202, AAR M128-B Steel.

FIGURES (continued)

10. Stress-Rupture Data for Three Plate Samples from Tank Car RAX 202, AAR M128-B Steel.
11. Stress-Ruptures Data for Three Plate Samples from Tank Car RAX 202, AAR M128-B Steel.
12. Stress-Rupture Data of Several Pressure Vessel Steels.
13. Hot-Tension Test Specimen No. 21, Plate Sample TC2-(11B).
14. Hot-Tension Test Specimen No. 38, Plate Sample TC2-(11B).
15. RTF Stress-Rupture Specimen No. 25, Plate Sample TC2-(11B).
16. RTF Stress-Rupture Specimen No. 32, Plate Sample TC2-(11B).
17. IRH Stress-Rupture Specimens.
18. Photomicrographs of Fracture Profile Sections Showing the Fracture Edge.
19. Photomicrographs of Fracture Profile Sections Showing the Fracture Edge.
20. Photomicrographs of the Region Immediately Behind the Fracture Surface.
21. Photomicrographs of the Region Immediately Behind the Fracture Surface.
22. Photomicrographs of the Region Immediately Behind the Fracture Surface.
23. SEM Fractographs of Selected Fracture Surfaces, Plate Sample TC2-(11B).
24. SEM Fractographs of Selected Fracture Surfaces, Plate Sample TC2-(11B).
25. SEM Fractographs of Selected Fracture Surfaces.



## ABSTRACT

Studies were undertaken at the National Bureau of Standards to measure the elevated-temperature mechanical properties and to determine the elevated-temperature fracture behavior of selected AAR M128-B steel plates taken from insulated tank car RAX 202. This tank car had been previously tested to failure in a fire environment. Further, these measured elevated-temperature mechanical properties were compared with published data of other plate samples of AAR M128-B steel. A secondary effort was to measure the ambient-temperature mechanical properties of plate samples taken from tank car RAX 202 to determine if the requirements of specification AAR M128-69-B were satisfied.

Three plate samples, designated TC2-(1), TC2-(3) and TC2-(11B), representing two shell courses, were selected for this study. The NBS results of check chemical analyses, hardness surveys, thickness measurements, macroscopic observations, and metallographic analyses of these three plate samples had been previously reported.

The results of ambient-temperature tensile tests showed that all three plate samples met the ultimate tensile strength, yield strength, and percent elongation requirements of specification AAR M128-69-B.

The results of hot-tensile tests showed a continuous decrease in ultimate tensile strength and yield strength, and an increase in tensile ductility, as measured by percent elongation, as the test temperature was increased from 1100 F to 1250 F. These results indicated that dynamic strain ageing was not significant in the temperature range investigated for the testing speeds used.

Analysis of stress-rupture data for specimens from all three plate samples in the temperature range of 1100 F to 1250 F indicated that a single straight line in a log-log plot of initial stress versus rupture life reasonably represented the data at each test temperature. This result appears to be independent of the plate sample or the specimen orientation. Further, in the temperature and stress range investigated, a decrease in the initial stress of approximately 20 to 30 percent resulted in a twelvefold increase in the rupture life from 15 minutes to three hours.

A comparison of the results of the metallographic analysis of hot-tensile and representative stress-rupture specimens in this study with the previously reported metallographic results on the initial rupture site in the failed shell course, all from tank car RAX 202, indicate the presence of the identical fracture mode. This mode is characterized by many intergranular voids which originate primarily at the proeutectoid ferrite-pearlite boundaries. These results confirm the previously reported finding that the initial rupture of tank car RAX 202 was a stress-rupture crack.

A comparison of hot-tensile and stress-rupture test results between specimens from tank car RAX 201 and specimens from tank car RAX 202 showed substantial disagreement. The steel plates used to

fabricate both tank cars were reportedly produced from the same heat of AAR M128-69-B steel, and thus the origin of the discrepancy in the elevated-temperature mechanical properties between specimens from these two tank cars is not apparent.

## 1. INTRODUCTION

In recent years, a number of catastrophic failures of railroad tank cars carrying hazardous materials have occurred. These catastrophic accidents have prompted the Federal Railroad Administration (FRA) to sponsor research activities with the object of developing knowledge concerning the various factors responsible for causing rupture and failure of tank cars involved in accidents, and to use this knowledge to prevent or minimize the effects of tank car failures.

In one phase of the FRA-sponsored research program, fire engulfment tests were conducted on two full-scale rail tank cars filled with liquified petroleum gas (LPG); uninsulated tank car RAX 201 and insulated tank car RAX 202. The steel plates used in the fabrication of both tank cars were reported to be 5/8 inch-thick, fine-grained steel plate in the as-rolled condition, produced to specification AAR M128-69, Grade B, Flange Quality, by Lukens Steel Company as part of Melt Number CO 485.(1) <sup>a</sup>

The fire tests on both full-scale tank cars were conducted at White Sands Missile Range, New Mexico, under the direction of personnel from the United States Army Ballistic Research Laboratory (BRL). The details of the test procedures and instrumentation used in these fire tests have been reported previously. (2,3) A metallurgical analysis of the failure of the uninsulated tank car, RAX 201, indicated that the initial rupture was the result of a stress-rupture crack which initiated near the top of the tank car. (4)

The FRA requested that the National Bureau of Standards (NBS) conduct a metallurgical evaluation of the failed insulated tank car, RAX 202. The analysis of the failure led to the conclusion that the initial rupture was a stress-rupture crack which formed as a result of prolonged exposure to elevated temperatures. (5)

The results of the two full-scale fire tests and data from other tank car failures (6) suggest that knowledge of the elevated-temperature mechanical properties of tank car steels is essential to any understanding of the failure behavior of tank cars carrying compressed gases subjected to fire environments. At present, however, elevated-temperature data available in the literature for AAR M128-B steel appears limited. Typical of the available data are results from hot-tensile tests on specimens from a failed tank car (7) and from an as-rolled plate (8), and hot-tensile tests and short-time stress-rupture tests on specimens from the fire tested uninsulated tank car, RAX 201 (4).

Accordingly, a program was initiated at NBS to measure the elevated-temperature mechanical properties of AAR M128-B steel plates used in the insulated tank car, RAX 202. Three plate samples, previously

---

<sup>a</sup> The isolated numbers in parentheses refer to references listed at the end of the report.

designated TC2-(1), TC2-(3) and TC2-(11B)<sup>b</sup>, representing two shell courses, were selected for this investigation. The NBS results of check chemical analyses, hardness surveys, thickness measurements, macroscopic observations, and metallographic analyses of these three plate samples have been previously reported. (5)

Plate sample TC2-(1), taken from the top of the failed shell course in the region experiencing the highest temperature during the fire test, contained a portion of the stress-rupture crack believed to have been the site of the initial rupture of the tank car. Plate sample TC2-(3) was removed from the bottom of the failed shell course in the region heated the least during the fire test. Plate sample TC2-(11B), taken from the bottom of the tank car in an unfailed shell course, was selected because it was located in an undeformed and relatively unheated region of the tank car. After the fire test, the bottom of the tank car still contained a portion of the original thermal protective coating which indicated that this region was heated the least during the test. A schematic of a portion of the tank car, Figure 1, shows a representation of the plate samples in their approximate locations, as viewed from the outside of the tank car.

## 2. PURPOSE

The principal purpose of this investigation was to determine the hot-tensile and short-time stress-rupture properties of AAR M128-B steel plates used in the fabrication of insulated tank car RAX 202 which had previously failed in a fire engulfment test. Another purpose was to determine the ambient temperature mechanical properties of these plates and to compare the properties with the requirements of specification AAR M128-69-B.

## 3. EXPERIMENTAL PROCEDURES

Forty-five specimens taken from plate samples TC2-(1), TC2-(3) and TC2-(11B) for ambient-temperature and hot-tensile tests, and for stress-rupture tests, were prepared in accordance with ASTM E8-69, Tension

<sup>b</sup> Plate sample TC2-(11) contained portions of the shell courses 1 and 2. Tests and observations on this plate sample are reported for the particular shell course involved; TC2-(11A) from shell course 2 and TC2-(11B) from shell course 1.

Testing of Metallic Materials.<sup>c</sup> The specimens, 0.250 inches in diameter in the reduced section with a one-inch-gage length, were taken as closely as possible from the quarterthickness position of the plate. Longitudinal and transverse specimens<sup>d</sup> were taken from plate sample TC2-(11B) while only longitudinal specimens were taken from plate samples TC2-(1) and TC2-(3). The location in the respective plate samples from which the test specimens were prepared are shown in Figures 2, 3 and 4. Macroscopic and metallographic observation were made on selected hot-tensile and stress-rupture specimens from plate samples TC2-(1), TC2-(3) and TC2-(11B).

### 3.1 Ambient-Temperature Tests

Eight specimens for ambient-temperature tensile tests were taken from plate samples TC2-(1), TC2-(3) and TC2-(11B) and tested in accordance with ASTM A370-73, Mechanical Testing of Steel Products. Two longitudinal and two transverse specimens were tested from plate sample TC2-(11B), and two longitudinal specimens were tested from each of the plate samples TC2-(1) and TC2-(3).

### 3.2 Elevated-Temperature Tests

Three test procedures were followed during the evaluation of the elevated-temperature mechanical properties.

#### 3.2.1 Resistance Heated Tube Furnace (RTF) Test Procedures

Hot-tensile tests and a limited number of stress-rupture tests were conducted using a three-zone resistance heated tube furnace with separate temperature control for each zone. The temperature of each zone was adjusted in order to minimize the temperature gradient along the specimen gage length. The maximum temperature gradient measured in the one-inch gage length was less than 6 F per inch. Three thermocouples were attached to each specimen, one on each shoulder and

<sup>c</sup> Four ASTM Recommended Practices are applicable to these three tests. Ambient temperature tension testing is covered by ASTM E8, Tension Testing of Metallic Materials. Hot-tensile testing is covered by ASTM E21, Elevated Temperature Tension Tests of Metallic Materials, and stress-rupture testing is covered by either ASTM E139, Conducting Creep, Creep-Rupture, and Stress-Rupture Tests of Metallic Materials or ASTM E150, Conducting Creep and Creep-Rupture Tension Tests of Metallic materials under Conditions of Rapid Heating and Short Times. The dimensions applicable to the standard 0.250 inch diameter, cylindrical test specimen are the same for each Recommended Practice with two exceptions. ASTM E21 and E139 require tighter tolerances on the gage length and diameter than the +/-0.005 inches required by ASTM E8 or E150. All specimens were prepared to a tolerance of +0.002 inches.

<sup>d</sup> Longitudinal and transverse refer to the longitudinal and transverse specimen axis orientation with respect to the principal plate rolling direction.

one at the center of the gage length. The specimen was placed in the center of the furnace, which had been preheated to the appropriate test temperature. The temperature of the specimen was monitored until the specimen reached thermal equilibrium at the test temperature.<sup>e</sup> The test was then initiated by the application of the load, and the specimen temperature was periodically monitored throughout the test. At the conclusion of each test, the specimen fragments were quickly removed from the furnace to avoid additional oxidation.

### 3.2.2 Internal-Resistance-Heating (IRH) Test Procedures

Stress-rupture tests were conducted using an alternative heating method based on the electrical resistance of the test specimen. A thermocouple attached to the specimen at the center of the gage length was used to maintain the appropriate test temperature by automatically controlling an electric current passing through the specimen. The ends of the specimen were clamped in water-cooled copper grips which resulted in a temperature gradient along the specimen gage length. The temperature gradient was believed to be substantially greater than that measured in the RTF method. The test terminated upon the fracture of the specimen which resulted in the breaking of the heating current circuit and the rapid cooling of the specimen fragments.<sup>f</sup>

### 3.2.3 Hot-Tensile Tests

Six longitudinal specimens prepared from plate sample TC2-(11B) were tested at temperatures of 1100 F, 1150 F, 1200 F, and 1250 F in accordance with ASTM E21-70, Elevated Temperature Tension Tests of Metallic Materials.<sup>9</sup> Four specimens, one at each test temperature, were tested at an initial crosshead speed of 0.005 inches per minute until yielding was complete. After yielding, the crosshead speed was gradually increased to 0.05 inches per minute for the remainder of the test. The other two specimens were tested, one at 1100 F and one at 1200 F, with the crosshead speed maintained at 0.05 inches per minute for the entire test.

---

<sup>e</sup> The time to reach thermal equilibrium varied between approximately 60 minutes to 75 minutes depending on the test temperature.

<sup>f</sup> When specimen necking occurs using the internal-resistance-heating method, the temperature of the specimen may increase above the nominal test temperature if the thermocouple is not located at the point of necking. Therefore, in this investigation, a meaningful test result was obtained if the fracture site and the thermocouple location are coincident.

<sup>9</sup> Exceptions to the procedure of E21 were as follows: (i) single specimens were tested at each temperature, (ii) the strain was calculated from the crosshead displacement.

### 3.2.4 Stress-Rupture Tests

Thirty-one specimens for stress-rupture tests were taken from plate samples TC2-(1), TC2-(3) and TC2-(11B): Fifteen longitudinal and six transverse specimens from plate sample TC2-(11B), four longitudinal specimens from plate sample TC2-(1), and six longitudinal specimens from plate sample TC2-(3). Tests were conducted at temperatures of 1100 F, 1150 F, 1200 F and 1250 F. Twenty-nine of the 31 specimens were tested by the internal-resistance heating technique (IRH) in accordance with E150-64, Conducting Creep and Creep-Rupture Tension Tests of Metallic Materials under Conditions of Rapid Heating and Short Times. The other two specimens were tested in an electric resistance tube furnace (RTF) in accordance with E139-70, Conducting Creep, Creep-Rupture, and Stress-Rupture Tests of Metallic Materials.

### 3.3 Macroscopic and Metallographic Observations

The exterior surfaces of five hot tensile specimens and three stress-rupture specimens were macroscopically examined after testing in both the optical microscope and the scanning electron microscope (SEM). Metallographic observations were made on fracture profile sections, taken parallel to the specimen axis, from one of the specimen halves from each of the six hot-tensile specimen and from eight of the stress-rupture specimens. SEM fractographs were taken of the fracture surfaces of the other half of the fourteen specimens used for the metallographic analyses.

## 4. RESULTS AND DISCUSSION

### 4.1 Ambient-Temperature Tensile Properties

The results of ambient-temperature tensile tests of specimens taken from plate samples TC2-(1), TC2-(3) and TC2-(11B) are given in Table I, along with the tensile property requirements for AAR M128-B-69 steel plates. These results show that, for all plates tested, the ultimate tensile strength values were within the specification limits of 81 to 101 ksi, and the yield strength and percent elongation values exceeded the minimum specification requirements of 50 ksi and 19 percent, respectively.

For plate sample TC2-(11B), the average values of longitudinal and transverse ultimate tensile strength were 85.9 and 86.3 ksi, respectively, and the average value of yield strength was 55.1 ksi for both orientations. These values indicate that there was little anisotropy in the strength of the plate in the plane of the rolling direction. However, the average tensile ductility values, measured by percent elongation, were 30.2 percent and 27.2 percent, respectively, for longitudinal and transverse specimens. Thus, the longitudinal elongation values were approximately ten percent higher than the transverse values. This finding was consistent with the general observation that the tensile ductility of rolled steel plates tends to be greater in the longitudinal direction than in the transverse direction.

A review of the ambient-temperature mechanical properties of three plate samples of AAR M128-B-65 steel and one plate sample of AAR M128-A-69 steel (9) shows: (i) Little difference between the average ultimate tensile strength and yield strength values of longitudinal and transverse specimens. (ii) The average longitudinal ductility, measured by percent elongation, was approximately ten percent higher than the transverse ductility. The anisotropy of tensile ductility observed in this study, as well as that observed in earlier work on plate samples taken from tank cars which failed under a variety of conditions, is attributed to the hot-rolling operation used to fabricate AAR M128 steel plates.

As shown in Table I, the average ultimate tensile strength value obtained from plate sample TC2-(3) was 87.3 ksi, as compared with 84.6 ksi for plate sample TC2-(1). The tensile ductility values for plate sample TC2-(3) were 26.6 percent elongation and 63.0 percent reduction-in-area, as compared with 29.6 percent elongation and 65.2 percent reduction-in-area for plate sample TC2-(1). Thus, specimens from plate sample TC2-(3) were found to exhibit a higher average ultimate tensile strength and lower average tensile ductility than specimens from plate sample TC2-(1). These results are consistent with observations and measurements previously reported (5) for plate samples TC2-(3) and TC2-(1). In the earlier work, it was found that plate sample TC2-(1), taken from the top of the tank car in the region experiencing the highest temperatures, was softer and contained a greater degree of iron carbide spheroidization than plate sample TC2-(3), taken from the bottom of the tank car in the least heated region.

The yield strengths for both specimens tested from plate sample TC2-(3) were unusually high, averaging 72.0 ksi, which was approximately 30 percent higher than the average values of 55.9 ksi and 55.1 ksi, respectively, for plate samples TC2-(1) and TC2-(11B). This observation, characteristic of the yield strength data, but not the tensile strength data, is possibly related to the plastic deformation which occurred in the region containing plate sample TC2-(3) as a result of the partial flattening of the fragment of shell course 3 immediately after the failure of tank car RAX 202. It is known that such plastic deformation may increase the yield strength, but not the tensile strength of ductile metals.

#### 4.1.1 Strain Ageing Effects

Strain ageing manifests itself in susceptible steels by the presence of a sharp yield point and by increases in flow stress, ultimate tensile strength, and hardness relative to the unstrain aged material. Peterson (10) studied the strengthening effects of strain ageing on low-(0.09 weight percent carbon) and medium-(0.46 weight percent carbon) carbon steels. The ambient-temperature tensile properties were measured on specimens that had been plastically deformed at temperatures up to 1000 F. Measured values of the 0.2-percent yield strength were up to

120 percent above the values for undeformed specimens and were accompanied by increases in ultimate tensile strength of up to 50 percent above the undeformed values for both the low- and medium-carbon steels.

Specimens tested from plate sample TC2-(3) did not exhibit sharp yield points<sup>h</sup> although small yield points were observed for all specimens tested from plate samples TC2-(1) and TC2-(11B), as shown in Table I. These observations are consistent with what is believed to be the previous thermal-mechanical history of these three plate samples. Plate sample TC2-(11B) was selected for this study because of its location in an undeformed and relatively unheated region of the tank car. This plate sample is believed to reasonably represent an aluminum deoxidized, hot-rolled plate of AAR M128-B steel in the stress-relieved condition. The observed small yield point in specimens from TC2-(11B) was not unexpected, since stress-relieving an aluminum deoxidized, hot-rolled carbon steel does not necessarily eliminate strain ageing effects (11). Further, the presence of yield points in specimens from plate sample TC2-(11B), representative of the tank car shell plates in the fabricated and stress-relieved condition, suggests that yield points should be observed in the other plate samples studied in this investigation. All of the plates used in tank car RAX 202 were rolled from the same heat of steel and would be expected to have the same strain ageing susceptibility. The presence of a yield point in specimens from plate sample TC2-(1) indicated that the effect of the fire exposure was insufficient to eliminate the yield point. Plate sample TC2-(3) was plastically deformed as a result of the catastrophic failure of the tank car and thus would be expected to exhibit a yield point if ageing occurred subsequent to the deformation or if the amount of plastic deformation was insufficient to eliminate the yield point. The absence of the yield point in specimens from TC2-(3) suggests that the deformation was sufficient to eliminate the yield point and that subsequent ageing effects were too small to produce a measurable yield point.

The high yield strength values measured on specimens from TC2-(3) are not believed to be the result of strain ageing for the following reasons. First, the absence of a measurable yield point indicates that the strain ageing effect would be too small to explain the magnitude of the increase in yield strength for specimens from TC2-(3) compared to specimens from TC2-(11B). Second, the large increase in yield strength was not accompanied by either a significant increase in ultimate tensile strength, as shown in Table I, nor an increase in hardness (5) compared to specimens from TC2-(11B).

#### 4.2 Hot-Tensile Properties

The results of the elevated-temperature tensile tests of specimens from plate sample TC2-(11B) are given in Table II and Figures 5 and 6.

<sup>h</sup> The tensile machine used for these tests was sufficiently stiff to allow observation of sharp yield points.

The results show, that for a given test procedure, there was a continuous decrease in ultimate tensile strength and yield strength and a continuous increase in percent elongation as the test temperature was increased from 1100 F to 1250 F. The percent reduction-in-area values, although less temperature sensitive than the strength or elongation values, showed a gradual increase as the test temperature was increased.

The ultimate tensile strength, measured at the slower crosshead speed of 0.005/0.05 inches per minute,<sup>1</sup> decreased from 29.9 ksi at 1100 F to 16.8 ksi at 1250 F, whereas the yield strength decreased from 20.7 ksi to 9.5 ksi over the same temperature interval. The tensile ductility values for these specimens were 39.2 percent and 46.5 percent, respectively, for percent elongation and percent reduction-in-area at 1100 F and 57.4 percent elongation and 53.7 percent reduction-in-area at 1250 F.

At the higher crosshead speed of 0.05 inches per minute, the ultimate tensile strength decreased from 34.1 ksi at 1100 F to 24.1 ksi at 1200 F, whereas the yield strength was 32.4 ksi at 1100 F and 21.1 ksi at 1200 F. The corresponding values for percent elongation and percent reduction-in-area were, respectively, 27.0 and 37.2 at 1100 F and 44.9 and 41.3 at 1200 F. The yield strength-to-ultimate tensile strength ratio at this higher crosshead speed was much greater than that at the lower crosshead speed (0.95 versus 0.69 at 1100 F and 0.87 versus 0.57 at 1200 F), due to the fact that yield strength is more rate sensitive than is tensile strength.

The observed tensile ductility behavior is consistent with conclusions reported by Smith (12) in a review of the elevated-temperature static properties of carbon steels. The ductility of the steels referred to by Smith, as measured by percent elongation and percent reduction-in-area, generally increased as the test temperature was raised above the maximum strain ageing temperature of 600 F.

The data show that with increasing test temperature, the ultimate tensile strength and yield strength values decrease monotonically, thus indicating that dynamic strain ageing probably did not affect these strength properties over the temperature range investigated. This conclusion is in agreement with work of Peterson (10) and Miller (11), who found that dynamic strain ageing effects on a large number of carbon steels were not observed in hot-tensile tests conducted above 600 F.

---

<sup>1</sup> The initial crosshead speed of 0.005 inches per minute was not held constant for the entire test. After loading past the yield, the crosshead speed was gradually increased to 0.05 inches per minute as allowed by ASTM E21. Thus a quantitative comparison of crosshead speed effects on the mechanical properties cannot be made as the effective crosshead speed of these tests is somewhere between 0.005 inches per minute and 0.05 inches per minute.

The data further show that the effect of strain rate or crosshead speed on tensile strength is somewhat greater as the temperature of deformation increases. At 1100 F, a specimen tested at a crosshead speed of 0.05 inches per minute had a tensile strength 14 percent greater than that of a specimen tested at a crosshead speed of 0.005/0.05 inches per minute. At 1200 F, the increase in tensile strength was 19 percent for these two crosshead speeds. These results are in agreement with the results of Miller, Smith and Kehl (13) who investigated the influence of strain rate on the strength of pearlitic carbon-molybdenum steel and found that crosshead speed had a larger effect on tensile strength at 1100 F than at 850 F.

#### 4.2.1 Comparison of Hot-Tensile Data for AAR M128 Steel

It is of interest to compare the hot-tensile data from this study with data from other investigators in order to assess the degree of similarity in behavior between the various sets of data. Hot-tensile data are available from other measurements of the elevated-temperature mechanical properties of AAR M128-B steel. However, these data appear to be limited to the results of hot-tensile tests from only three other investigations: Three specimens from a fragment of the uninsulated tank car, RAX 201, were tested at 900 F, 1050 F and 1200 F (4), ten specimens from a fragment of tank car GATX 89971 from the Laurel, Mississippi accident were tested from room temperature to 1200 F (7), and three pairs of specimens from an as-rolled and stress-relieved plate were tested at 930 F, 1110 F and 1290 F (8).<sup>j</sup> The temperature dependence of the ultimate tensile strength and yield strength data from these three studies (only tensile strength data available for tank car RAX 201), together with the results of this investigation, are shown in Figures 7 and 8. Large variations in tensile and yield strengths for identical temperatures are apparent: Comparing the data of plates taken from failed tank cars, the values from tank cars RAX 201 and RAX 202 are the highest and lowest, respectively, and the values from tank car GATX 89971 are intermediate.

The strong effect of strain rate (or crosshead speed) on elevated-temperature tensile properties necessitates that details of the test procedure must be stated before a precise comparison of data can be made. The strain rate used in two of the other three investigations was not reported; however, the tests on specimens from tank car GATX 89971 were reportedly conducted in accordance with established procedures and by appropriate ASTM specifications. The tests on the normalized and stress-relieved specimens, which were prepared from as-rolled plate, were

---

<sup>j</sup> Six additional specimens from another as-rolled plate, identified as AAR TC128-B steel, were tested at the same three temperatures in the normalized condition. However, the reported check chemical analysis for this plate revealed sufficient vanadium to classify this plate as a TC128-A steel and thus were not included for comparison in this report.

reportedly conducted at strain rates of 0.5 percent per minute and five percent per minute for the determination of the 0.2-percent yield strength and ultimate tensile strength, respectively. These testing rates are identical to those used in the current study, if it is assumed (as an approximation) that crosshead speed is a suitable basis for calculating strain rate.

A comparison of ultimate tensile strength data from the normalized and stress-relieved specimens with the results of this investigation on specimens in the as-rolled and stress-relieved condition shows excellent agreement over the temperature range studied. The agreement between the yield strength data is not as good as that of the tensile strength data, possibly as a result of using crosshead displacement measurements in this study to compute the 0.2-percent strain. The overall agreement between the strength data of the normalized and stress-relieved specimens compared to the as-rolled and stress-relieved specimens is good and is consistent with observations by other investigators. Miller (11) reported that for the same nominal composition and ferrite grain size, the tensile strengths of the carbon steels that he investigated were comparable, whether made to coarse- or fine-grain practice or whether in the as-rolled or stress-relieved condition.

In addition to the strain-rate effects on elevated-temperature strength properties, variations in ambient-temperature strength properties may also result in similar variations of elevated-temperature strength properties. Smith (12) concluded that, in general, elevated-temperature tensile and yield strength vary as the ambient values and, to a first approximation, the former can be predicted from the latter in some cases. The reported ambient-temperature ultimate tensile and yield strength values of specimens from GATX 89971 were approximately 95.0 ksi and 63.5 ksi, respectively, compared to 85.9 ksi and 55.1 ksi, respectively, for plate sample TC2-(11B), which was tested in this investigation. Therefore, the elevated-temperature tensile and yield strength values for specimens from GATX 89971 would be expected to be higher than those for specimens from TC2-(11B) and this is consistent with the values actually measured.

Surprisingly, the largest difference in the tensile strength data, which were available for comparison, occurs between results from the uninsulated tank car, RAX 201, and the insulated tank car, RAX 202, both of which were reportedly fabricated from the same heat of AAR M128-B steel. At 1200 F, the tensile strength of the plate sample from RAX 201 was about 49 ksi, which is more than twice that of plate sample TC2-(11B) from RAX 202. Although the ambient-temperature strength properties for the plate sample from RAX 201 were not reported, these properties are not expected to be significantly different from those of RAX 202. Differences in the rate of testing could account for the large difference in ultimate tensile strength values. However, the rate of testing for the specimens from tank car RAX 201 would have to have been exceptionally high and well outside of ASTM recommended practices. Thus, large differences in the measured values of the elevated-temperature tensile strength of specimens taken from plates fabricated from the same heat of steel and tested at two different laboratories are not readily explainable.

### 4.3 Stress-Rupture Properties

The results of stress-rupture tests conducted on specimens prepared from plate samples TC2-(1), TC2-(3) and TC2-(11B) are given in Table III. The data are grouped by test temperature and are plotted in the traditional form of the logarithm of the initial stress as a function of the logarithm of the time-to-rupture, as shown in Figures 9a, 9b, 10a and 11. Each temperature group contains the results of specimens from each plate sample and orientation tested by either of the two stress-rupture test techniques, described earlier in Sections 3.2.1 and 3.2.2. The data at each test temperature were analysed by a least-squares technique, and the resulting calculated line was plotted with the individual data points as shown in the graphs.

Inspection of each graph reveals that, at each test temperature, a single straight line adequately represents all of the data, and the linear relationships are independent of plate sample location and specimen orientation. Further, there is no evidence of a change in slope in the stress versus time-to-rupture curves for the data presented.<sup>k</sup> The single straight lines, obtained in the current study at each test temperature, indicate that specimen oxidation was not significant, and that a single fracture mode was probably operative.

The results obtained using the IRH technique were verified by two stress-rupture tests conducted with a conventional resistance tube furnace (RTF). These tests were conducted at 1200 F at two stress levels on longitudinal specimens from plate sample TC2-(11B). These results are included in Table III. A log-log plot of the data obtained with the IRH method on longitudinal specimens from plate sample TC2-(11B) is shown in Figure 10b. Superimposed on the plot are the two RTF test results showing that the agreement between the two heating techniques is good and that for the stress levels and temperatures used in this study, the IRH technique will produce reliable time-to-rupture data.

#### 4.3.1 Comparison of Stress-Rupture Data for Tank Car Steels

The amount of stress-rupture data on tank car steels such as ASTM A212 or AAR M128 found in the literature is rather limited (4, 16).

<sup>k</sup> A change-in-slope or a break in the linear behavior for many alloys can sometimes be correlated with a change in the fracture mode, and such behavior has been reported for carbon steels and low-alloy steels. (14) However, a change-in-slope does not always indicate a change in fracture mode. The results of White, Clark, and Wilson (15) for a carbon steel demonstrated that the observed break in the stress versus rupture time curves was a consequence of oxidation of the test specimens. Protection of the specimens against the oxidizing atmosphere (air) resulted in a linear relationship for the test conditions studied. The stress levels used in the present study were sufficiently high so that the rupture times were much shorter than those reported by White, et al.

One investigation (16) of the stress-rupture properties of a plate of ASTM A212 steel was carried out at 1000 F and at stresses such that the minimum rupture time was about four hours. The only data reported for AAR M128-B steel (4) consists of seven stress-rupture tests conducted on specimens taken from the uninsulated tank car, RAX 201. In the analysis of the data from tank car RAX 201, the investigators assigned a rupture life of 0.03 hours (1.8 minutes) to the three hot-tensile tests and combined these three data points with the seven stress-rupture data points to make a total of ten data points.

In the current study, the data from tank car RAX 201 were analysed by a least-squares technique and plotted together with the results of this study on tank car RAX 202, as shown in Figure 12. A comparison of the data obtained from specimens taken from plates fabricated from the same heat of steel and tested at two different laboratories shows large differences in measured values of stress-rupture strength: The stress-rupture strength values at 1200 F reported in earlier work (4) on a plate sample from tank car RAX 201 are much greater than those for plate samples from tank car RAX 202 tested in the present study. These differences are as striking as the differences in the elevated-temperature tensile strength values which were discussed in Section 4.2.1 of this report.

Smith (12), in his review of carbon steels, concluded that the scatter of elevated-temperature rupture strength values obtained from nominally identical carbon steel plates was substantial and that these differences in rupture strength values are partially associated with differences in composition and manufacturing practice allowable under current specifications. However, the results of previously reported check chemical analyses for the plate samples from tank car RAX 202 (5) indicated a high degree of chemical homogeneity not only between different areas within a plate sample and between different plate samples, but also between these check chemical analyses and the producer's ladle analysis. Although check chemical analyses were not reported for any plate sample from tank car RAX 201, significant differences in chemical composition between the two tank cars would not be expected. Thus, it is highly probable that the differences in stress-rupture strength values between specimens from tank car RAX 201 and specimens from tank car RAX 202 are not a result of compositional variations.

The absence of ambient-temperature mechanical property data from a relatively unheated and undeformed region of tank car RAX 201 precludes a determination as to whether there may have been differences in the fabrication procedure or stress-relieving practice between the two tank cars. However, since these two tank cars were fabricated specifically for the Tank Car Safety Program, it is unlikely that substantial variations in the fabrication and/or heat treatment procedures occurred.

Finally, there remains the possibility that the significant variations in these elevated-temperature mechanical properties are the

result of differences in the rupture environment seen by the plate samples tested. Apart from this last speculation, however, there appears to be no explanation for the substantial differences in elevated-temperature mechanical properties observed between specimens from tank car RAX 201 and specimens from tank car RAX 202.

#### 4.4 Macroscopic and Metallographic Analyses

Macroscopic examination of the hot-tensile test specimens and selected stress-rupture test specimens revealed that the specimen surface, within the reduced cross-section, contained irregular, secondary cracks adjacent to and parallel to the fracture surface. These cracks were, in general, perpendicular to the applied stress. The hot-tensile specimens and the RTF stress-rupture specimens contained many secondary surface cracks in a region up to approximately 0.5 inches on either side of the fracture surface on a given specimen. The IRH stress-rupture specimens, however, contained comparatively fewer secondary surface cracks and the cracks were limited to a region approximately 0.1 inches on either side of the fracture surface. These differences are believed to be a result of the higher temperature gradient existing in the IRH specimens.

Optical photographs, Figures 13a, 14a, 15a and 16a, and SEM photographs, Figures 13b, 14b and 15b, show that the secondary cracks are distributed around the specimen circumference and become larger and more numerous as the fracture surface is approached.

Representative photomicrographs of fracture profile sections are shown in the unetched condition in Figures 13c, 14c, 15c, 16b and 17. The extensive development of internal voids or cracks is apparent in the vicinity of the fracture surface. The voids in the IRF stress-rupture specimens are limited to a smaller specimen volume than the voids found in the hot-tensile specimens or the RTF stress-rupture specimens; this behavior is analogous to the secondary surface crack observations discussed earlier.

Photomicrographs taken on fracture profiles are shown in the etched condition in Figures 18 and 19a. Large numbers of voids or cracks can be seen, as well as a general elongation of proeutectoid ferrite grains in the direction of the applied stress. Higher magnification photomicrographs, Figures 20, 21 and 22a, were taken of the region directly behind the fracture surface. These photomicrographs show that the voids are intergranular or interphase in character since they are located primarily at the boundaries between the proeutectoid ferrite grains and the pearlite. Often, these voids appear to form as a result of a pulling apart (or separation) of the ferrite grains from the pearlite, as seen in Figure 20b.

SEM fractographs were taken of representative fracture surfaces of hot-tensile and stress-rupture specimens; cracks or voids in the fracture surface are shown in Figure 23. At higher magnifications,

Figures 24 and 25a, the generally dimpled character of the fracture surface is revealed, indicative of ductile fracture.

Macroscopic observations of the region believed to be the site of the initial rupture in the insulated tank car, RAX 202, (5) revealed that, on both plate surfaces near this portion of the fracture, numerous small secondary cracks were present and they were aligned parallel with the fracture surface and perpendicular to the principal tensile or hoop stress direction in the tank car. The majority of these surface cracks were confined to a region of within one-half- to one-inch of the fracture surface, where most of the decrease in plate thickness (or thinning) occurred. Metallographic examination indicated that the rupture was initiated by cracks or voids which formed primarily at interfaces between proeutectoid ferrite and pearlite, as shown in Figures 19b and 22b. An SEM fractograph, Figure 25b, showed the dimpled character of the fracture surfaces as well as the presence of voids.

A comparison of the results from the analysis of representative test specimens from this study with the results of a similar analysis of the region believed to be the site of the initial rupture in insulated tank car RAX 202, shows a high degree of similarity between the features observed on and near the fracture surfaces. Both investigations revealed the presence of secondary surface cracks, interphase voids, and a generally dimpled fracture surface indicating ductile fracture.

#### 4.5 General Discussion

The purposes of this investigation were several fold. The primary effort was to measure the elevated-temperature mechanical properties and to determine the elevated-temperature fracture behavior of selected AAR M128-B steel plates taken from the insulated tank car, RAX 202. Further, these elevated-temperature properties were to be compared with the published properties of other plate samples of AAR TC128-B steel. A secondary effort was to measure the ambient-temperature mechanical properties of plate samples taken from tank car RAX 202 to determine if the requirements of specification AAR M128-69-B were satisfied.

For these studies, three plate samples representing two shell courses were selected: a) plate sample TC2-(1), taken from the top of the tank car in the failed shell course, shell course 3, b) plate sample TC2-(3), taken from the bottom of the tank car in the failed shell course, and c) plate sample TC2-(11B), taken from the bottom of the tank car in a shell course that did not fail, shell course 1. All of the steel plates used to fabricate tank car RAX 202 were reportedly produced from a single heat of steel.

#### 4.5.1 Ambient-Temperature Properties

Ambient-temperature mechanical properties were determined from longitudinal specimens taken from plate samples TC2-(1), TC2-(3) and TC2-(11B). The measured values of ultimate tensile strength, 0.2-percent yield strength, and percent elongation from all specimens tested met the requirements of specification AAR M128-69. In addition, check chemical analyses of the three plate samples, previously reported (5), also met the requirements of AAR M128-69. The average values of tensile strength, yield strength, and percent elongation, 86.0 ksi, 55.5 ksi and 28.8 percent, respectively, compare favorably with the average values of 87.0 ksi, 56.7 ksi, and 30.6 percent, respectively, reported for longitudinal specimens from a shell course sample of AAR M128-B-65 steel taken from another failed tank car. (17)

#### 4.5.2 Hot-tensile Properties

The results of the hot-tensile tests indicated a behavior consistent with that observed in a large number of carbon steels. The decreasing ultimate tensile and yield strengths with increasing test temperature indicated that dynamic strain ageing was not a significant effect for the specimens tested in the temperature range of 1100 F to 1250 F. However, strain rate or crosshead speed effects were observed in this temperature range; the measured values of ultimate tensile strength and yield strength increased and the measured values of tensile ductility decreased as a result of increasing the strain rate. These strain rate effects reflect the fact that with increasing strain rate (or crosshead speed), the strengthening effects of hot-strain hardening are relatively greater than the thermal softening effects.

A comparison of the elevated-temperature tensile strength values for plate samples reportedly produced to specification AAR M128-B from two of three failed tank cars, tank car GATX 89971 (7) and tank car RAX 202 in the present study, and an as-rolled plate (8), shows a maximum variation in ultimate tensile strength in the temperature range 1100 F to 1250 F of 26 to 40 percent, respectively; the maximum variation at 1100 F was 29 ksi to 36.5 ksi and at 1250 F, the variation was 20 ksi to 28 ksi. However, specification AAR M128-B allows a variation in the ambient-temperature ultimate tensile strength of up to 25 percent above the minimum specified value, from 81 ksi to 101 ksi, and the typical variation in testing speeds used in the temperature range of the present study can result in differences in tensile strength of another 10 to 20 percent; 29.9 ksi to 34.1 ksi at 1100 F and 20.3 ksi to 24.1 ksi at 1200 F. Thus, the observed variation in elevated-temperature tensile strength values for these three plate samples appears to be consistent with the variation in ambient-temperature tensile strength allowed by specification AAR M128-B, and with the effect of testing speed on the elevated-temperature tensile strength.

The one exception in the agreement between hot-tensile strength data from various sources is the data representing a plate sample from the uninsulated tank car, RAX 201 (4). The large difference in ultimate tensile strength between the sample from RAX 201 and the other plate samples from RAX 202 is difficult to understand. The discrepancy between the data from tank cars RAX 201 and RAX 202 is all the more puzzling because both tank cars were reportedly fabricated from plates produced from a single heat of steel. The plate samples from RAX 202 met both the chemical requirements and ambient-temperature strength and tensile ductility requirements of specification AAR M128-69-B, and there is no reason to believe that the steel plates in RAX 201 failed to meet these specification requirements.

The elevated-temperature tensile strength values reported for tank cars RAX 201 (4), RAX 202 (this study), and GATX 89971 (7) were determined for plate samples taken from tank cars which had failed in fire environments. The evidence reported in these studies suggests that plate sample TC2-(11B) from RAX 202 and the plate sample from GATX 89971 were taken from portions of the respective tank cars which were heated the least (if at all) by the fire exposure. The plate sample taken from RAX 201, however, was located near the top of the tank car and contained what is believed to be the site of the initial rupture. The available evidence indicates that the top of the tank car experienced the highest temperatures during the fire test (2), and thus it is possible that this plate sample could have been affected by both the elevated temperature and the deformation associated with the subsequent rupture and failure of the tank car.

A comparison of ambient-temperature tensile properties and elevated-temperature rupture properties can be made, however, between heated and relatively unheated plate samples from tank car RAX 202. The ambient-temperature tensile properties and elevated-temperature rupture properties measured on specimens from plate sample TC2-(1), taken from the top of the failed shell course and containing a portion of the initial rupture, were not significantly different from the values representative of plate sample TC2-(11B), taken from the bottom of the tank car in an unfailed shell course. This evidence suggests that the properties of the plate sample from RAX 201 were probably not affected by the elevated temperature and subsequent rupture and failure of the tank car. The lack of information on the ambient-temperature mechanical properties and the hot-tension-test procedures followed in conducting tests of the specimens from RAX 201 makes it difficult to comment on the reason or reasons why these tensile strength data depart widely from the consistent data from plate samples from the other three tank cars.

The design and specifications for a variety of pressure vessels involve a burst pressure parameter which can be calculated from the design equations of the vessel. These equations are used to compute the burst pressure from the geometry of the vessel and from materials properties such as the ultimate tensile strength. The results

of the comparison made in this report between a limited number of sets of hot-tensile data suggest that significant variations in the hot-ultimate-tensile strength exist for steel plates produced to the AAR M128-69-B specification. This variation is sufficiently large so that hot-tensile-strength data from a single plate sample are probably inadequate as a basis for calculating tank car burst pressures at elevated-temperatures. Other investigators (4), using one set of data (7) previously reported, have computed a tensile design curve of tank car burst pressure as a function of temperature<sup>1</sup>. However, the data represented only the hot-tensile strength data from a single plate sample from a tank car, GATX 89971, which failed as a result of a derailment and subsequent fire. Thus, the calculated burst pressure-temperature curve would not necessarily describe the expected behavior of tank cars fabricated from different AAR M128-B steel plates.

The knowledge of the mechanical properties of a specific sample of a structural material is not an adequate basis upon which to design a structure using this material. The usefulness of any data in the prediction of the anticipated behavior of a material depends on whether or not the data is representative of different samples of a material produced to the same specification. The comparison made in this of the limited amount of hot-tensile data available suggests that a tensile design curve of tank car burst pressure versus temperature cannot be presently calculated in the temperature range of 1100 F to 1250 F.

#### 4.5.3 Stress-Rupture Properties

In the present study, the results of the short-time stress-rupture tests were in good agreement with the results of the hot-tension tests. The ultimate tensile strength values of specimens taken from plate sample TC2-(11B), measured from tests using controlled crosshead speeds, were equivalent to rupture lifetimes, uncorrected for strain rate effects, of approximately 0.16 hours or less in the temperature range of 1100 F to 1250 F. Other investigators have correlated ultimate tensile strength values with rupture lifetimes. White, et al, (15) found that for a carbon steel, the tensile strength values in the temperature range of 1200 F to 1300 F corresponded to rupture lifetimes of 0.15 hours or less. Thus, in the current study, the equivalent rupture lifetimes of the elevated-temperature tensile strength values of specimens from plate sample TC2-(11B) are consistent with the equivalent rupture lifetimes reported for a carbon steel.

The results of the least-squares analyses of the stress-rupture data indicate that a single straight line reasonably represents all of the data for each test temperature irrespective of the specimen

---

<sup>1</sup> The question as to what equations are appropriate for calculating the elevated-temperature burst pressure are not discussed in this report.

orientation or the plate sample from which the specimens were taken. Neither the effect of the fire environment on plate sample TC2-(1) nor the deformation received by plate sample TC2-(3) was apparently sufficient to cause a measurable difference in their short-time stress-rupture properties compared to the average stress-rupture properties of all specimens tested at each test temperature. In addition, the stress-rupture strength values of the transverse specimens from plate sample TC2-(11B) were not measurably different from the stress-rupture strength values of the longitudinal specimens from the three plate samples. This latter observation is consistent with the finding that there is little difference in the ambient-temperature strength properties of the longitudinal and transverse specimens from TC2-(11B).

The absence in the literature of stress-rupture data for AAR M128-B steel plates makes it difficult to establish whether or not the data measured in this study are representative of this grade of steel. A comparison of the stress-rupture data from the plate sample from tank car RAX 201 with the data from tank car RAX 202, measured in this study, revealed the same large variance in rupture strength values as the previously discussed variance between the respective hot-tensile strength data from these two tank cars. The stress-rupture data and hot-tensile data of each tank car are self-consistent, and thus the origin of this discrepancy in elevated-temperature mechanical properties between nominally identically steel plates is not apparent.

Stress-rupture data for another widely used tank car steel, ASTM A212 steel, was found to be very limited. The time-to-rupture curve for a sample of ASTM A212 steel tested at 1000 F, shown in Figure 12, was drawn by graphically extrapolating the data reported by Smith (16) from lower stress levels to higher stress levels. The rupture strength values for AAR M128-B steel in the temperature range investigated in the present study are consistent with the data taken from a single plate of a similar tank car steel, ASTM A212.

Stress-rupture data taken at 1100 F for a low-carbon boiler-plate steel (18) were also included in Figure 12. The boiler-plate steel contained 0.13, 0.27 and 0.03 weight percent carbon, molybdenum, and columbium, respectively, as compared to the specification requirement of 0.25 and 0.08 maximum weight percent carbon and molybdenum, respectively, for AAR M128-B steel plates. The increased stress-rupture strength of the boiler-plate steel as a result of the molybdenum addition is apparent, even though the reported ambient-temperature tensile strength value of this boiler-plate steel is approximately 70 ksi as compared to a minimum of 81 ksi for AAR M128-B steel.

In the current study, the rupture lifetime was observed to be strongly dependent on the initial applied stress level, in the temperature and stress ranges investigated. By extrapolation of the stress-rupture data from this study, shown in Figure 12, to longer rupture times, with the longest extrapolation being less than a factor of ten in lifetime, it can be shown that a 20 percent decrease in the 15-minute-lifetime stress

at 1100 F would cause a twelvefold increase in the rupture life from 15 minutes to three hours. Similarly, a 30 percent decrease in the 15-minute-lifetime-stress at 1150 F, 1200 F and 1250 F would result in the same twelvefold increase in the rupture lifetime. The insulated tank car, RAX 202, remained intact for approximately one and one-half hours before failure, although the time during which the top of the tank car experienced temperatures in excess of 1000 F is estimated to be less than 30 minutes<sup>m</sup>. Although changes in the metallurgy of tank car steels through selected alloy additions can substantially enhance the stress-rupture strength by increasing the rupture lifetimes at higher stress levels than can be attained with AAR M128-B steel, a significant increase in rupture life for AAR M128-B steel can be achieved by reducing the time during which the tank car experiences the maximum internal pressure or reducing the maximum internal pressure<sup>n</sup>. Reducing the internal pressure by using additional relief valves, larger flow capacity relief valves, or lower opening pressure relief valves appear to be possible approaches to increasing the elevated-temperature rupture lifetime requirement of tank cars.

#### 4.5.4 Metallographic Analysis

The results of the metallographic analyses in this study show the presence of the same fracture mode in both the hot-tension specimens and the stress-rupture specimens. This fracture mode is characterized by the presence of irregular, secondary surface cracks lying perpendicular to the applied stress direction and by large numbers of interphase cracks or voids in the region immediately behind the fracture surface. These voids originate primarily at the boundaries between the proeutectoid ferrite and the pearlite. SEM fractographs of the fracture surface reveal the presence of these voids and confirm the ductile character of the fracture surface by the presence of dimples. The primary cause of failure is the formation of these numerous cavities or cracks, although at the instant of catastrophic failure, transgranular fracture of some proeutectoid ferrite grains may occur.

The observation that single-slope lines can reasonably be fitted to the stress-rupture data for each test temperature is consistent with the metallographic findings of a single fracture mode in the stress-rupture specimens. The observation of the same fracture

---

<sup>m</sup> Approximately 60 minutes after the beginning of the fire test on RAX 202, the instrumentation system recording temperature and pressure data failed. The maximum temperature recorded at the time of the instrumentation loss was 850 F. If the rate of temperature increase remained constant for the remainder of the test, from 60 to 94 minutes, then an extrapolation of the temperature-time data would show that the time during which the temperature exceeded 1000 F would be close to 15 minutes.

<sup>n</sup> A typical relief-valve-opening pressure of 250 psig is equivalent to a maximum wall stress, calculated using the Bach equation (19), of about 20 ksi.

mode in both hot-tensile and stress-rupture specimens is not unexpected, since most of the stress-rupture tests were conducted at initial stress levels that were close to or above the yield strength of the steel at the test temperature.

The characteristics of the fracture mode observed in both the hot-tensile tests and the stress-rupture tests are the same as those observed in specimens taken from what is believed to be the initial rupture site in the insulated tank car, RAX 202. These results further support the earlier findings (5) that the features of the initial rupture region in the insulated tank car are characteristic of failure by a stress-rupture mechanism.

## 5. SUMMARY

1. For this investigation, three steel plate samples, designated TC2-(1), TC2-(3) and TC2-(11B), were taken from an insulated tank car, RAX 202, which failed while subjected to a fire environment. Test specimens were taken from these plates for ambient-temperature tensile tests, hot-tensile tests, and stress-rupture tests. Metallographic observations were made on selected specimens after testing.

2. These plate samples were removed from two shell courses. Two samples were taken from shell course 3, the only shell course that fractured: TC2-(1), which contained what is believed to be the site of the original rupture near the top of the tank car; and TC2-(3), located at the bottom of the tank car, which was relatively unaffected by the fire exposure. The third sample, TC2-(11B), was taken from a relatively undeformed and unheated region at the bottom of the tank car in a shell course that did not fail, shell course 1. Plate sample TC2-(11B) was believed to be representative of the as-fabricated steel plates used in tank cars RAX 201 and RAX 202, which were reportedly produced from the same heat of steel.

3. Ambient-temperature tensile tests conducted on longitudinal specimens from plate samples TC2-(1), TC2-(3) and TC2-(11B) showed that all three plate samples met the ultimate tensile strength, yield strength, and percent elongation requirements of specification AAR M128-69-B. Yield strength values for specimens from TC2-(3) were approximately 30 percent higher than the levels for plate samples TC2-(1) and TC2-(11B). The increase is believed to be the result of a small amount of plastic deformation which occurred in this plate sample as a result of the failure of the tank car and the expulsion of shell course 3 out of the test pit.

4. Ambient-temperature tensile tests conducted on longitudinal and transverse specimens from plate sample TC2-(11B) showed little anisotropy in the strength properties in the plane of the rolling direction. Tensile ductility values, as measured by percent elongation, showed that the longitudinal elongation values were approximately ten percent higher than the transverse elongation values.

5. Hot-tensile tests conducted at 1100 F, 1150 F, 1200 F and 1250 F on longitudinal specimens from plate sample TC2-(11B) showed a continuous decrease in ultimate tensile strength and yield strength, and an increase in percent elongation as the test temperature was increased. The percent reduction-in-area values were less temperature dependent than the percent elongation values, showing a pronounced increase only above 1200 F.
6. Results of tests at a testing rate of 0.05 inches per minute showed increases in ultimate tensile strength and yield strengths and decreases in percent elongation and percent reduction-in-area values, when compared with the values found for tests at an initial testing speed of 0.005 inches per minute.
7. If the effects of testing speed and differences in ambient-temperature strengths are taken into account, the results of the hot-tensile tests from this study are in good agreement, with one exception, with the results from other studies of AAR M128-B steel plates.
8. Stress-rupture data measured at 1100 F, 1150 F, 1200 F and 1250 F on longitudinal specimens from plate samples TC2-(1) and TC2-(3) and on longitudinal and transverse specimens from plate sample TC2-(11B) were analysed by at least-squares technique. A single-slope line in a log-log plot of initial stress versus rupture time represented the data at each test temperature. This result appears to be independent of the plate sample or specimen orientation.
9. The results of the stress-rupture tests indicate that in the temperature and stress range investigated, decreases in the initial stress level of approximately 20 to 30 percent result in a twelvefold increase in the rupture lifetime from 15 minutes to three hours.
10. Stress-rupture tests conducted with a resistance tube furnace (RTF) to heat the specimens indicated that tests conducted with an internal-resistance-heating (IRH) technique gave reliable time-to-rupture data at the stress levels and temperatures used in this study.
11. Little stress-rupture data on AAR M128-B steel were found in the literature for comparison with the results of this investigation. In the one instance where comparable data were found, reasonable agreement was obtained in a comparison of the present results with data from a related tank car steel, ASTM A212, which was tested at 1000 F.
12. A comparison of results from hot-tensile and stress-rupture tests on a plate sample taken from the uninsulated tank car, RAX 201, with those taken from the insulated tank car, RAX 202, showed substantial disagreement. The steel plates used to fabricate both tank cars reportedly were produced from the same heat of steel, and thus the origin of the wide variance in elevated-temperature properties between these samples is not explainable.

13. The results of the metallographic analysis of hot-tensile and representative stress-rupture specimens and the previously reported results on the initial rupture in the failed shell course, all from tank car RAX 202, indicate the presence of the identical fracture mode in all three types of metallographic samples. This mode is characterized by the presence of many interphase (intergranular) cracks or voids in the region immediately behind the fracture surface. The voids originate primarily at the proeutectoid ferrite-pearlite boundaries. SEM fractographs revealed the generally ductile character of the fracture surface by the presence of dimples which resulted from void nucleation and coalescence. These results confirm the previously reported findings that the initial rupture of tank car RAX 202 was a stress-rupture crack.

## 6. CONCLUSIONS

1. The variation in the ambient-temperature ultimate tensile strength allowed by specification AAR M128-B and the effect of the rate of testing can result in a significant variation in the elevated-temperature strength properties. The lack of substantial elevated-temperature mechanical property data in the literature appears to preclude the development, at the present time, of a design or trend curve for the variation of burst pressure with temperature for AAR M128-B steel. Knowledge of the lower bound to the burst pressure-temperature curve for AAR M128-B would be useful in the evaluation of existing relief-valve design.
2. The rupture life of AAR M128-B steel, as measured by uniaxial stress-rupture tests in the temperature range of 1100 F to 1250 F, is a strong function of both temperature and applied stress. Therefore, modifications of tank car technology which would either reduce the temperature dependence of the properties of the steel or reduce the maximum stresses and/or time at maximum stress experienced by the pressurized tank cars, could be important in efforts to reduce the possibility of a tank car failing catastrophically when subjected to a fire environment.
3. The results of the hot-tensile tests indicate that dynamic strain ageing in AAR M128-B steel is not significant in the temperature range and at the testing speeds used in this investigation.
4. In general, there were few differences in the measured ambient- and elevated-temperature mechanical properties between plate samples regardless of whether or not the plate sample was from the most or least heated regions of tank car RAX 202.

## 7. ACKNOWLEDGEMENT

The author wishes to express thanks to Drs. C. G. Interrante and B. W. Christ for their helpful comments and suggestions, and to Mr. D. E. Harne for his excellent contributions to the metallographic

and photographic portions of this report. In addition, thanks to Mr. C. H. Brady for his skillful and timely assistance with the scanning electron microscopy portion of this report. Special thanks are extended to Dr. W. F. Savage and Mr. John Lippold, Materials Engineering Department, Rensselaer Polytechnic Institute, for conducting the stress-rupture tests using the IRH technique.

## REFERENCES

1. Test Certificate, Lukens Steel Company, Mill Order Number 64931 1, Melt C0485, AAR-TC-128 GR. B, APPENDIX M FLG. 81000, February 29, 1972.
2. C. Anderson, W. Townsend, J. Zook, and G. Cowgill, "THE EFFECTS OF A FIRE ENVIRONMENT ON A RAIL TANK CAR FILLED WITH LPG," B.R.L. Interim Memorandum Report No. 288, USA Ballistic Research Laboratories, Aberdeen Proving Ground, Maryland, September 1974.
3. W. Townsend, C. Anderson, J. Zook, and G. Cowgill, "COMPARISON OF THERMALLY COATED AND UNINSULATED RAIL TANK CARS FILLED WITH LPG SUBJECTED TO A FIRE ENVIRONMENT," B.R.L. Interim Memorandum Report No. 319, USA Ballistic Research Laboratories, Aberdeen Proving Ground, Maryland, December 1974.
4. C. Anderson and E. B. Norris, "FRAGMENTATION AND METALLURGICAL ANALYSIS OF TANK CAR RAX 201," B.R.L. Interim Memorandum Report No. 213, USA Ballistic Research Laboratories, Aberdeen Proving Ground, Maryland, April 1974.
5. J. G. Early and C. G. Interrante, "A METALLURGICAL INVESTIGATION OF A FULL-SCALE INSULATED RAIL TANK CAR FILLED WITH LPG SUBJECTED TO A FIRE ENVIRONMENT," Report No. 7, NBSIR 75-657, January 1975.
6. "PHASE 01 REPORT ON SUMMARY OF RUPTURED TANK CARS INVOLVED IN PAST ACCIDENTS," Report RA-01-2-7, Railroad Tank Car Safety Research and Test Project, Association of American Railroads, Chicago, Illinois, July 1, 1972.
7. P. Gordon and D. L. Albright, "METALLURGICAL EVALUATION OF SAMPLES FROM TANK CARS DERAILED AT LAUREL, MISSISSIPPI," Appendix A, AAR Report No. MR-453 AAR Research Center, Chicago, Illinois, July 1969.
8. A. P. Coldren, Report ISJ-669, Climax Molybdenum Company, June 9, 1972.
9. C. G. Interrante, J. G. Early and G. E. Hicho, "ANALYSIS OF FINDINGS OF FOUR TANK-CAR ACCIDENT REPORTS," Report No. 5, NBSIR 75-655, January 1975.
10. J. L. Peterson, "STRAIN HARDENING IN HYPOEUTECTOID STEELS," Trans. ASM, 56, 304, 1963.
11. R. F. Miller, "THE STRENGTH OF CARBON STEELS FOR ELEVATED-TEMPERATURE APPLICATIONS," ASTM Proc., 54, 964, 1954.
12. G. V. Smith, "ELEVATED TEMPERATURE STATIC PROPERTIES OF WROUGHT CARBON STEELS," ASTM, STP 503, 1972.

13. R. F. Miller, G. V. Smith, and G. L. Kehl, "INFLUENCE OF STRAIN RATE ON STRENGTH AND TYPE OF FAILURE OF CARBON-MOLYBDENUM STEEL AT 850, 1000 AND 1100 DEGREES FAHR.," Trans. ASM, 31, 817, 1943.
14. T. Prnka and V. Foldyna, "THE CREEP PROPERTIES OF LOW-ALLOY Cr-Mo-V STEELS WITH LOW CARBON CONTENT," High-Temperature Properties of Steels, Proceedings of a BISRA-ISI Joint Conference, ISI Publication 97, 1967.
15. A. E. White, C. L. Clark and R. L. Wilson, "THE FRACTURE OF CARBON STEELS AT ELEVATED TEMPERATURES," Trans. ASM, 25, 863, 1937.
16. G. V. Smith, "AN EVALUATION OF THE ELEVATED TEMPERATURE TENSILE AND CREEP-RUPTURE PROPERTIES OF WROUGHT CARBON STEEL," ASTM Data Series, DS1151, 1970.
17. C. G. Interrante, G. E. Hicho, and D. E. Harne, "A METALLURGICAL ANALYSIS OF ELEVEN STEEL PLATES TAKEN FROM A TANK CAR ACCIDENT NEAR CALLAO, MISSOURI," Report No. 4, NBS Report 312.01/51, September 19, 1972.
18. T. Wada, "CREEP RUPTURE PROPERTIES, RESISTANCE TO TEMPER EMBRITTLEMENT AND TO HYDROGEN ATTACK OF A Mn - 0.25% Mo-Cb STEEL," Report RP-32-71-02, Climax Molybdenum Company, January 31, 1973.
19. J. M. Barsom and S. T. Rolfe, "FATIGUE AND BURST ANALYSIS OF HY-140(T) STEEL PRESSURE VESSELS," Jour. Eng. Ind. (Trans. ASME, Series B), 92, 11, 1970.

TABLE I. Ambient-Temperature Tensile Properties of Specimens Taken From Tank Car RAX 202

Plate Identification	Shell Course No.	Specimen Number and Orientation(a)	Tensile Strength, Ksi	Yield Strength 0.2%, Ksi	Elongation, % (b) in 1-inch-gage length	Percent Reduction in area, %	Presence of Sharp Yield Point
TC2-(1)	3	5-Long	85.6	58.1	29.1	62.4	Yes
		7-Long	83.5	53.7	30.0	67.9	Yes
		Average	84.6	55.9	29.6	65.2	
TC2-(3)	3	12-Long	88.0	74.3	24.7	61.9	No
		15-Long	86.7	71.5	28.4	64.0	No
		Average	87.3	72.9	26.6	63.0	
TC2-(11B)	1	66-Long	86.3	55.2	29.3	63.8	Yes
		64-Long	85.5	55.0	31.1	65.8	Yes
		Average	85.9	55.1	30.2	64.8	
TC2-(11B)	1	58-Trans.	83.6	55.9	26.4	55.1	Yes
		53-Trans.	84.0	54.3	27.9	53.9	Yes
		Average	86.3	55.1	27.2	54.5	

Specification AAR TC128-B-69

Max. 101.0  
Min. 81.0

Min. 50.0 Min. 19.0(c) (d)

- (a) Long. and trans. refer to the longitudinal and transverse specimen axis orientation with respect to the principal rolling direction of the plate.
- (b) Percent elongation in one-inch-gage length.
- (c) AAR TC128-B-69 requires a minimum elongation of 19% in two-inch-gage length. A comparison of elongation data obtained from different sizes of specimens of the same material can be made provided the ratio of the gage length to cross-sectional dimensions is held constant. Since the ratio of the square root of the cross-sectional area to the gage length is the same for the specimen with a 0.500-inch-diameter with a 2-inch-gage and for the specimen with a 0.250-inch-diameter with a 1-inch-gage length, the elongation data from the 1-inch-gage length specimen can be directly compared to the specification requirement based on a 2-inch-gage length.
- (d) Not specified.

TABLE II Hot-Tensile Properties of Specimens Taken From  
Plate Sample TC2-(11B)

Specimen Number and Orientation (a)	Test Temperature, F	Test Crosshead Speed, Inches/ Minute	Ultimate Tensile Strength, Ksi	Yield Strength (b) 0.2%, Ksi	Percent Elongation, (c) %	Percent Reduction in Area, %
21-Long	1100	0.0005(d)	29.9	20.7	39.2	46.5
62-Long	1100	0.05(e)	34.1	32.4	27.0	37.2
27-Long	1150	0.005	25.6	19.6	42.9	48.1
38-Long	1200	0.005	20.3	13.7	49.0	46.9
36-Long	1200	0.05	24.1	21.1	44.9	41.3
28-Long	1250	0.005	16.8	9.5	57.4	53.7

- (a) Long. and Trans. refer to the longitudinal and transverse specimen axis orientation with respect to the principal rolling direction of the plate.
- (b) The 0.2% offset yield strength was determined from a load-extension graph with the extension measured from the crosshead displacement.
- (c) Percent elongation in one-inch-gage length.
- (d) In accordance with ASTM E21, the crosshead speed was maintained at 0.005 inches per minute through the yield strength after which the crosshead speed was slowly increased to 0.05 inches per minute.
- (e) The crosshead speed was maintained at 0.05 inches per minute through the test.

TABLE III Stress-Rupture Properties of Specimens  
Taken From Tank Car RAX 202

Specimen Number and Orientation(a)	Plate Identification	Shell Course No.	Test Temperature, F	Stress Ksi	Time To Rupture, Hours
11-L	TC2-(3)	3	1100	22.3	2.16
37-L	TC2-(11B)	1	1100	26.1	0.05
40-L	TC2-(11B)	1	1100	21.5	2.18
31-L	TC2-(11B)	1	1100	21.5	1.79
44-L	TC2-(11B)	1	1100	20.0	1.92
4-L	TC2-(1)	3	1150	20.1	1.21
20-L	TC2-(3)	3	1150	22.5	0.40
16-L	TC2-(3)	3	1150	20.0	0.76
42-L	TC2-(11B)	1	1150	22.5	0.26
29-L	TC2-(11B)	1	1150	20.0	0.26
39-L	TC2-(11B)	1	1150	20.0	0.43
46-T	TC2-(11B)	1	1150	20.0	1.11
52-T	TC2-(11B)	1	1150	17.0	2.88
6-L	TC2-(1)	3	1200	18.9	0.27
3-L	TC2-(1)	3	1200	17.5	0.73
13-L	TC2-(3)	3	1200	17.6	0.84
14-L	TC2-(3)	3	1200	14.8	1.52
33-L	TC2-(11B)	1	1200	19.9	0.20
30-L	TC2-(11B)	1	1200	17.4	0.49
43-L	TC2-(11B)	1	1200	15.6	1.04
32-L(b)	TC2-(11B)	1	1200	17.5	0.36
25-L(b)	TC2-(11B)	1	1200	19.5	0.19-0.23(c)
57-T	TC2-(11B)	1	1200	18.5	0.41
2-L	TC2-(1)	3	1250	17.5	0.09
19-L	TC2-(3)	3	1250	15.9	0.16
45-L	TC2-(11B)	1	1250	20.0	0.05
26-L	TC2-(11B)	1	1250	17.4	0.19
41-L	TC2-(11B)	1	1250	14.4	0.37
55-T	TC2-(11B)	1	1250	17.4	0.10
56-T	TC2-(11B)	1	1250	15.9	0.15
54-T	TC2-(11B)	1	1250	12.2	0.95

(a) L and T refer to the longitudinal and transverse specimen axis orientation with respect to the principal rolling direction of the plate.

(b) Stress-rupture test conducted in a resistance - tube furnace (RTF).

(c) Load accidentally reduced for brief time just before the end of the test so that the true time to failure is not known. True time to failure must lie between actual time to rupture of 0.23 hours and time at which the full load was operative, 0.19 hours.

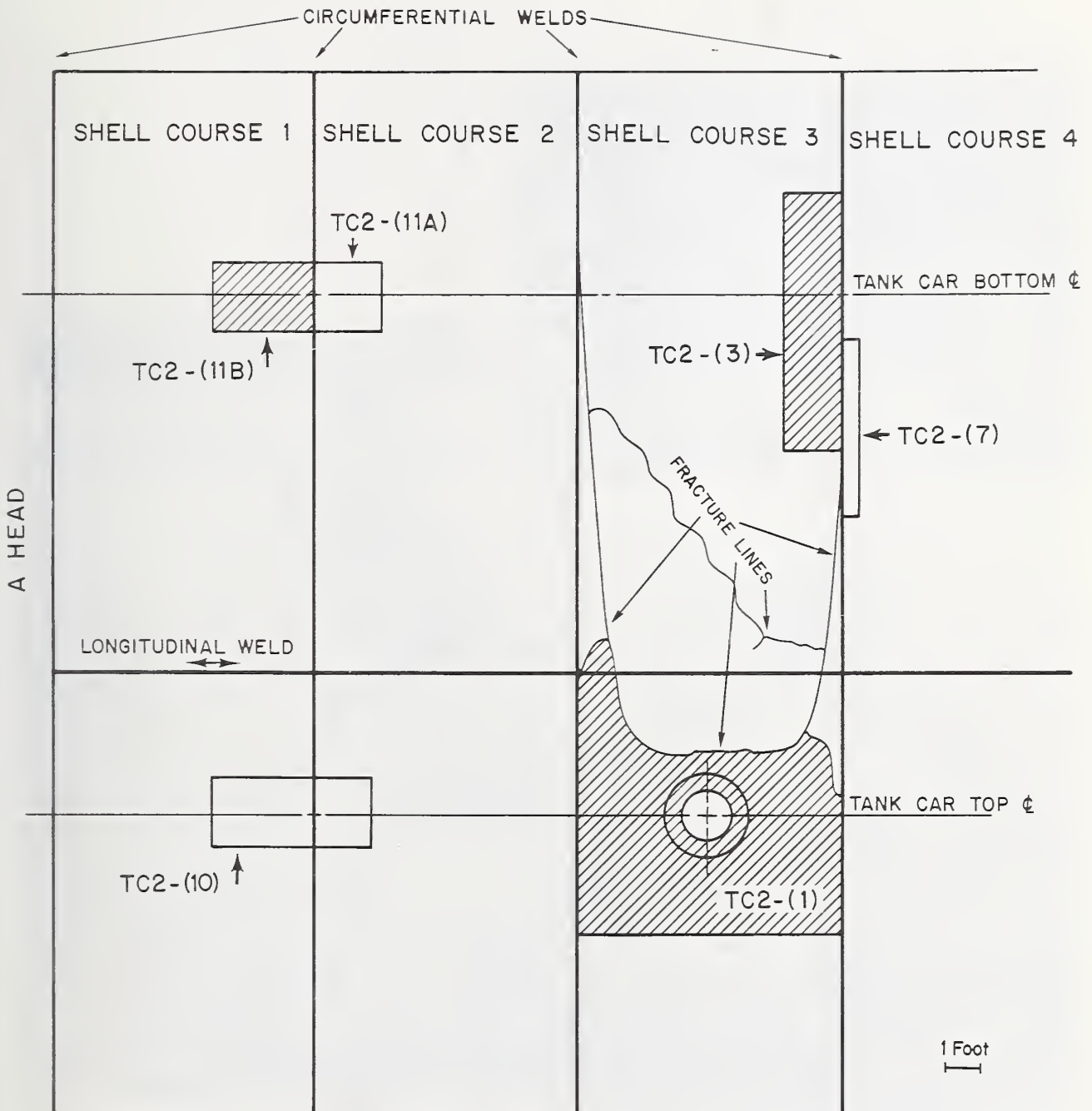


Figure 1. Schematic Diagram Showing the location of NBS Samples in Tank Car RAX 202 as Viewed from the Outside of the Tank Car.

The specimens used in this study were taken from the plate samples marked as .



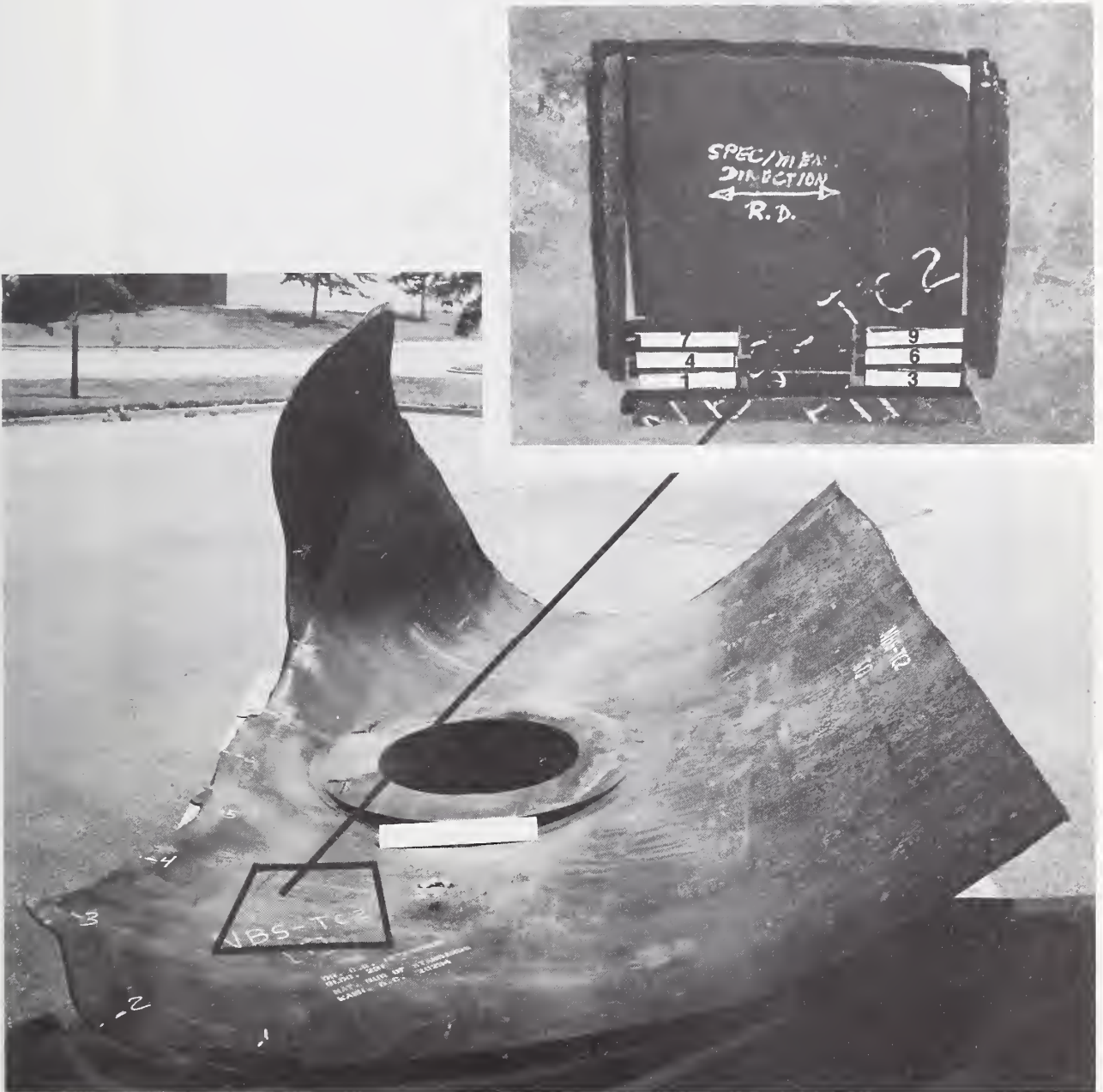


Figure 2. Plate Sample TC2-(1), Shell Course 3

Photograph shows the inside plate surface at the top of the tank car. The inset photograph shows the location from which the test specimens were removed. The white rectangles identify the test specimens and show the orientation of the specimens. Mag. X 1/12



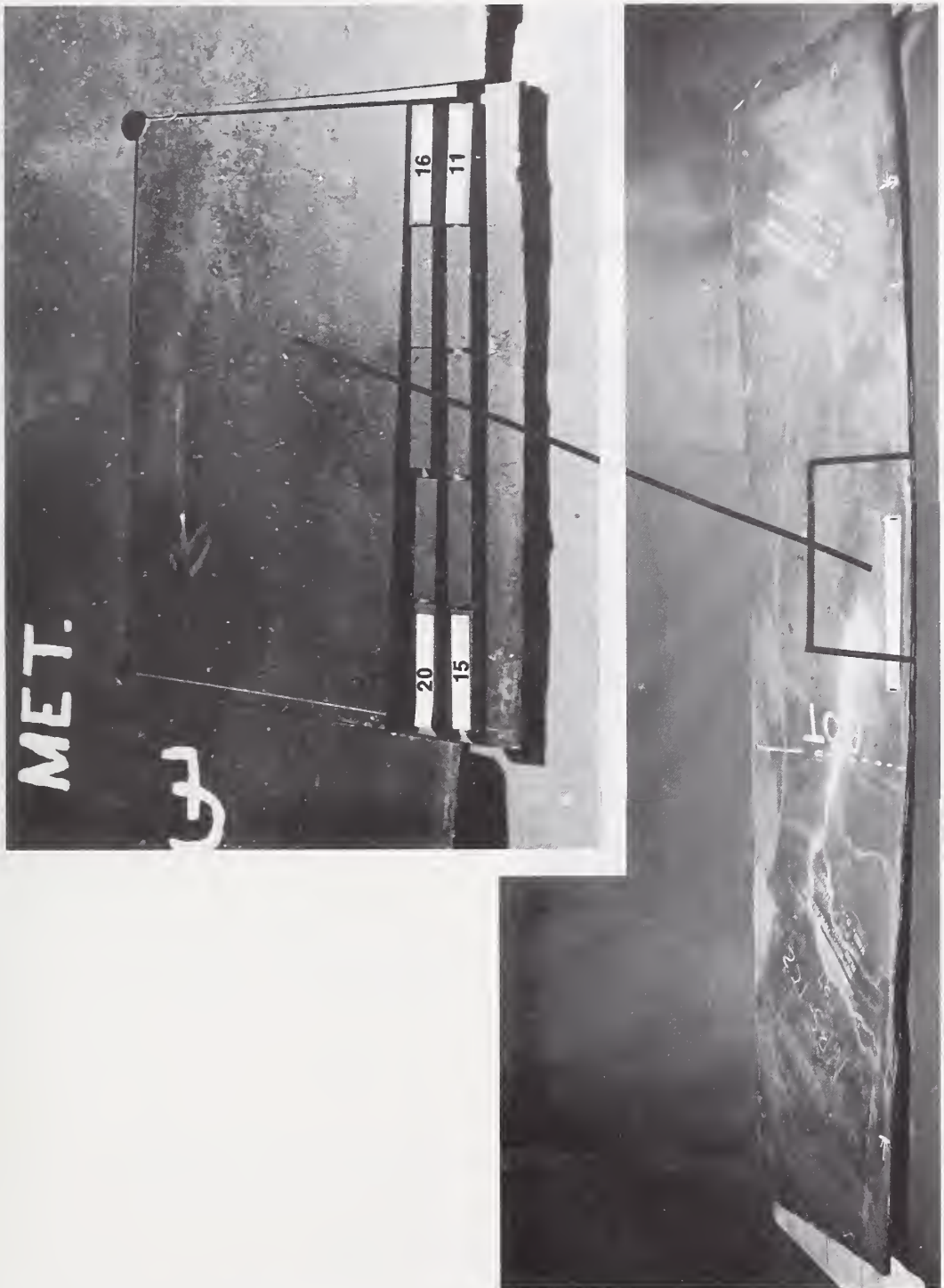


Figure 3. Plate Sample TC2-(3), Shell Course 3

Photograph shows the inside plate surface with the bottom center line of the tank car marked BOT. The inset photograph shows the location from which the test specimens were removed. The white rectangles identify the test specimens and show the orientation of the specimens. Mag. X 1/12





Figure 4. Plate Sample TC2-(11), Shell Course 1 and Shell Course 2. Photograph shows the outside plate surface at the bottom of the tank car. Plate sample TC2-(11A), shell course 2, is marked A and plate sample TC2-(11B), shell course 1, is marked B. The white rectangles identify the area from which the test specimens were removed and show the orientation of the specimens. Mag. X 1/12



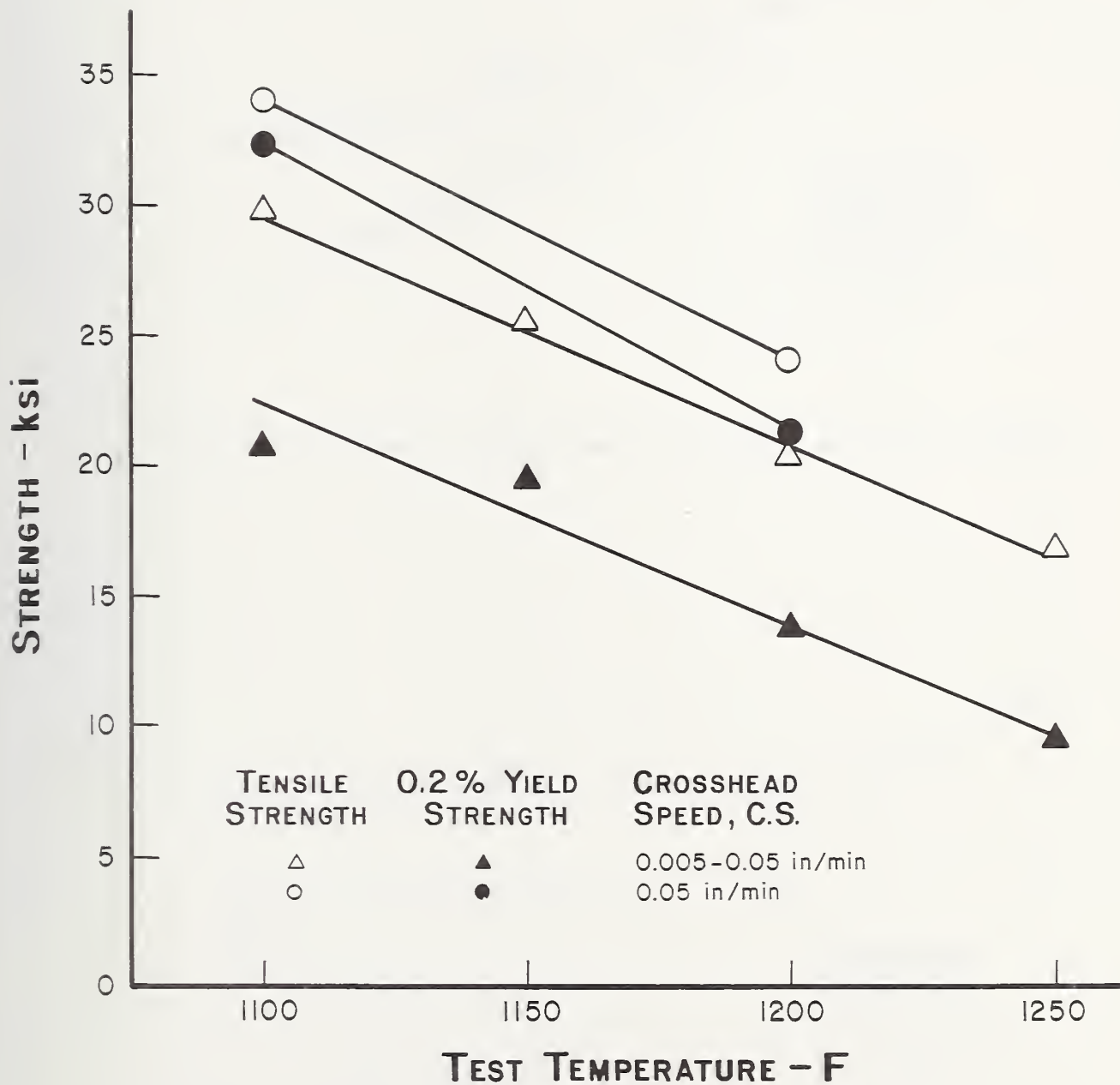


Figure 5. Elevated Temperature Strength Properties of Plate Sample TC2-(11B), AAR M128-B Steel, Taken from Tank Car RAX 202.



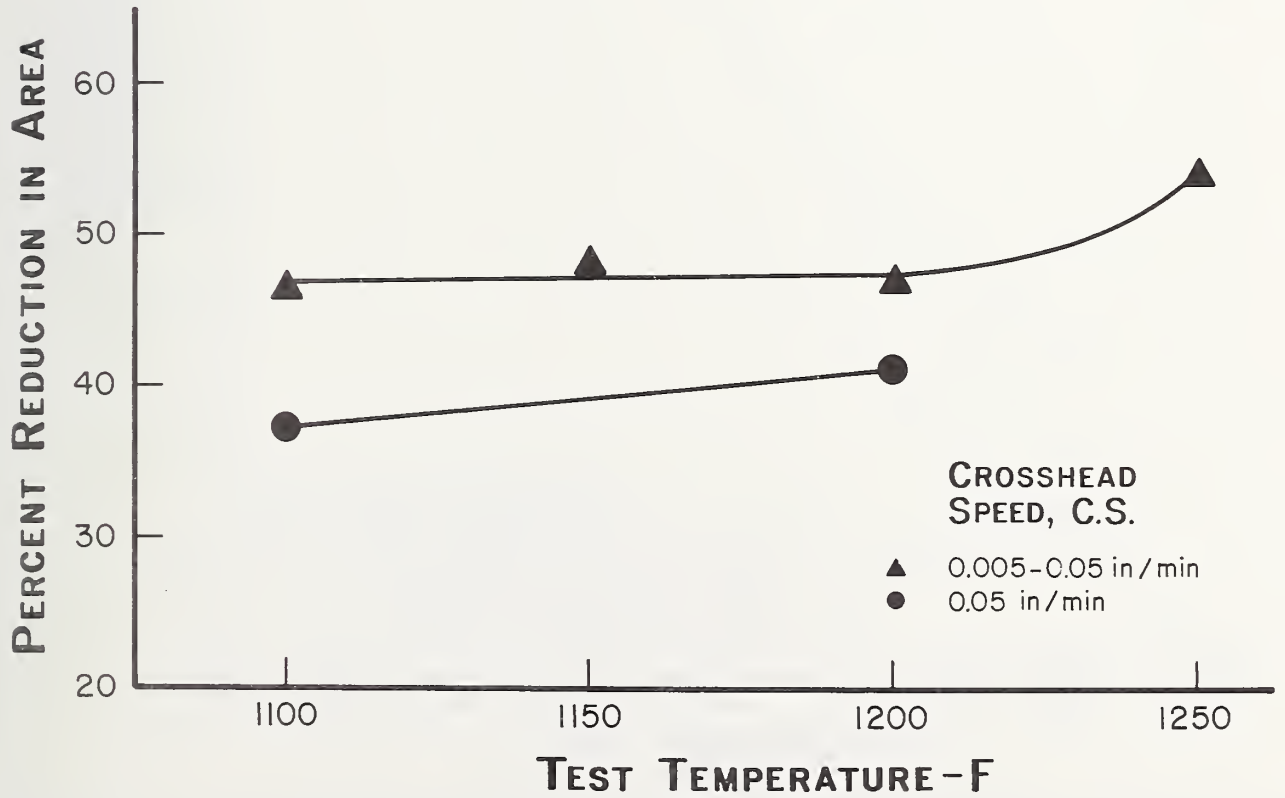
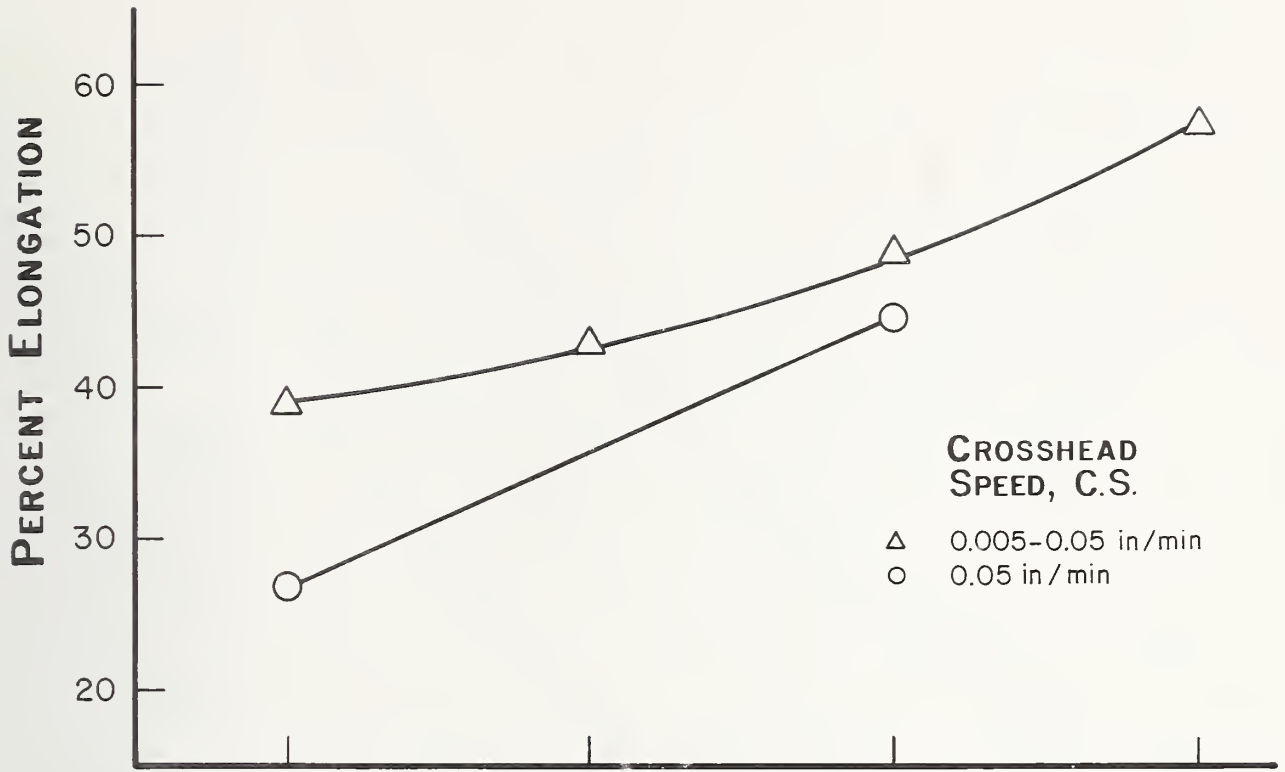


Figure 6. Elevated Temperature Tensile Ductility Properties of Plate Sample TC2-(11B), AAR M128-B Steel, Taken from Tank Car RAX 202.



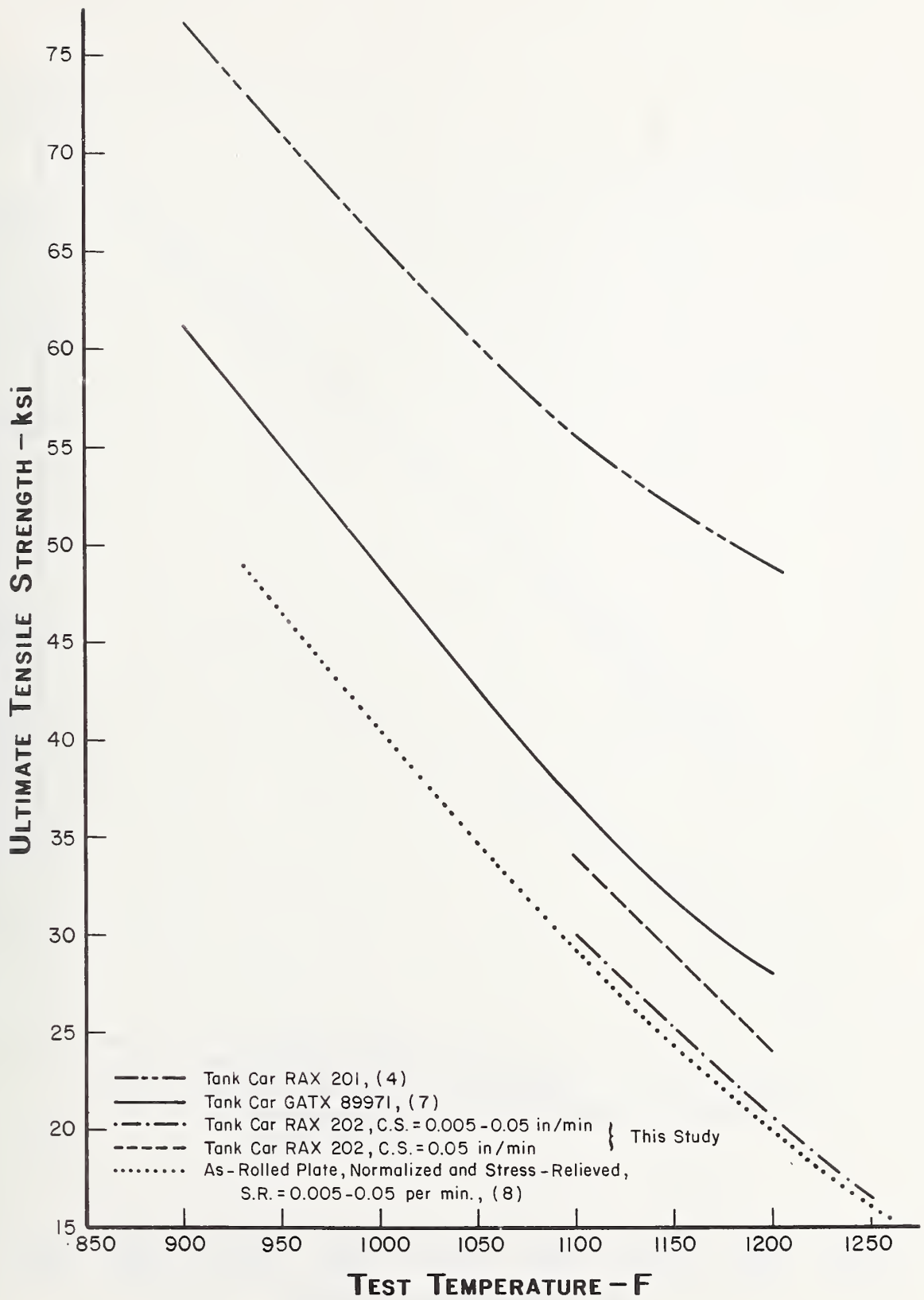


Figure 7. Elevated Temperature Ultimate Tensile Strength Properties of AAR M128-B Steel.



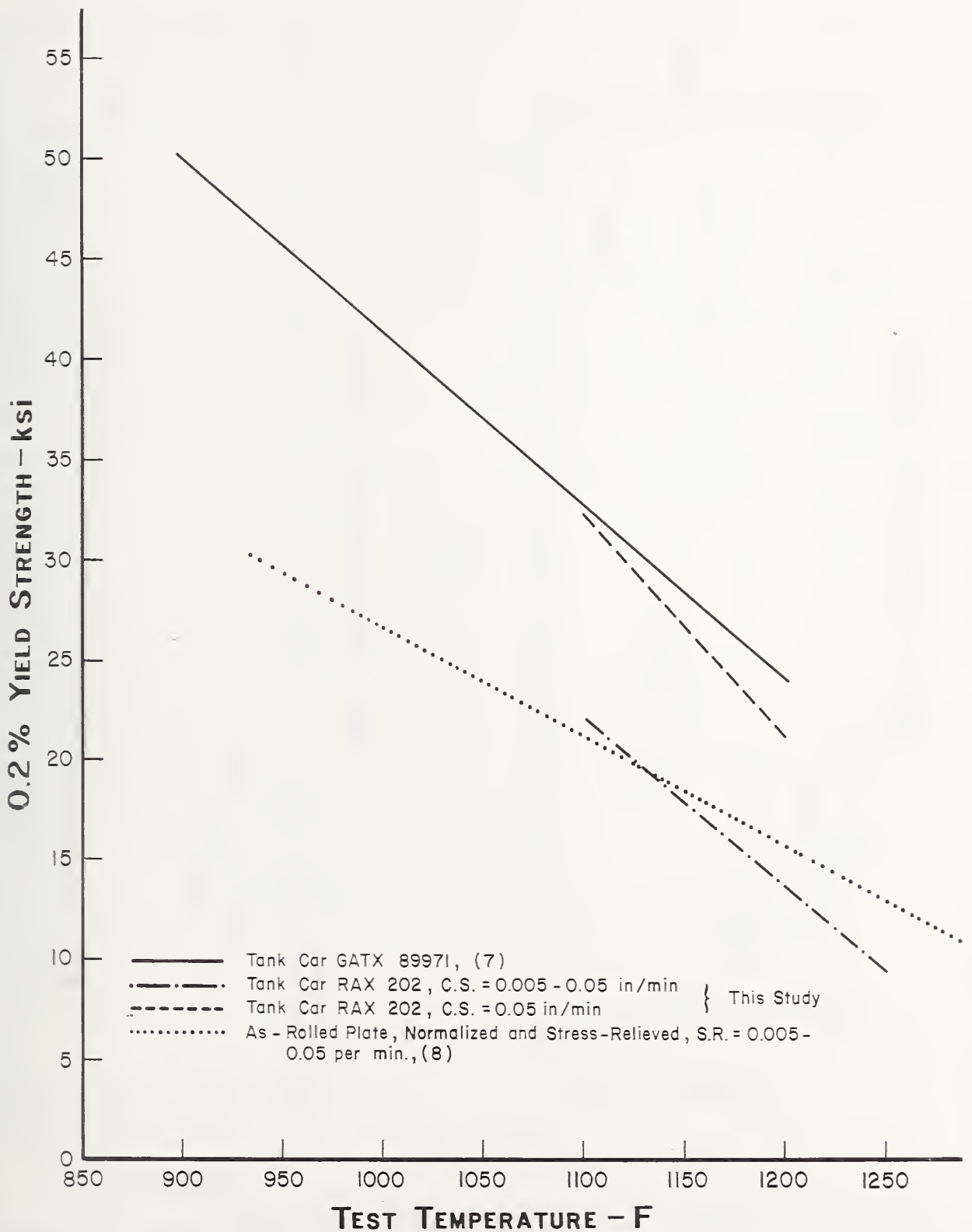
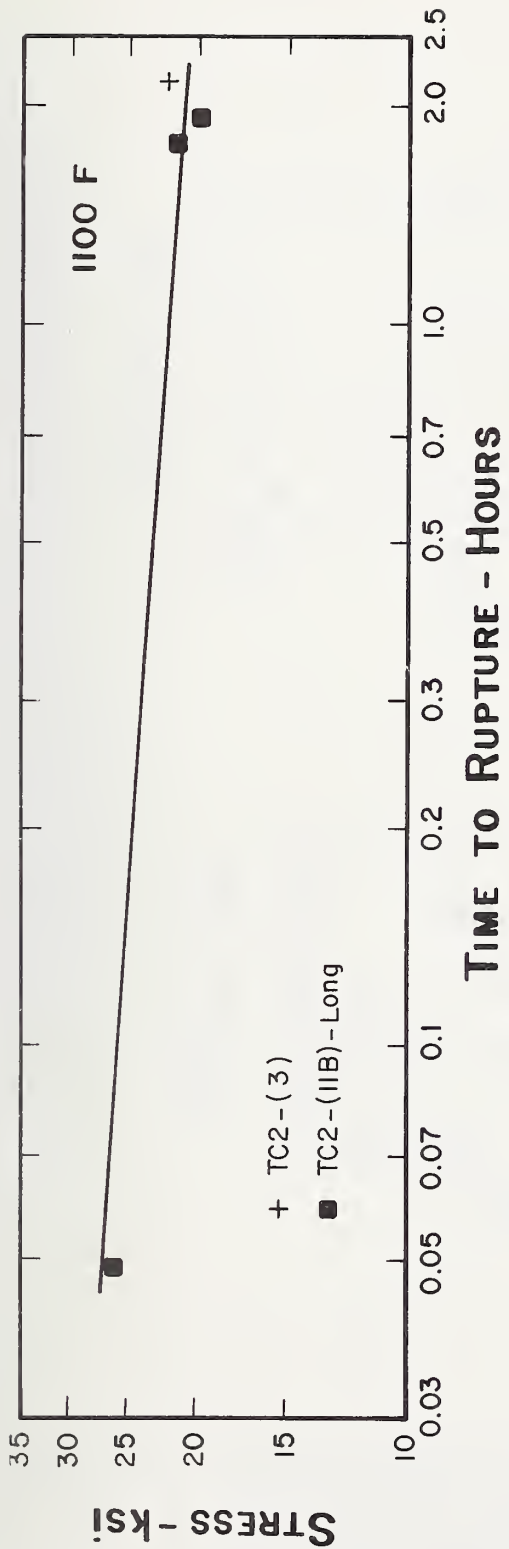
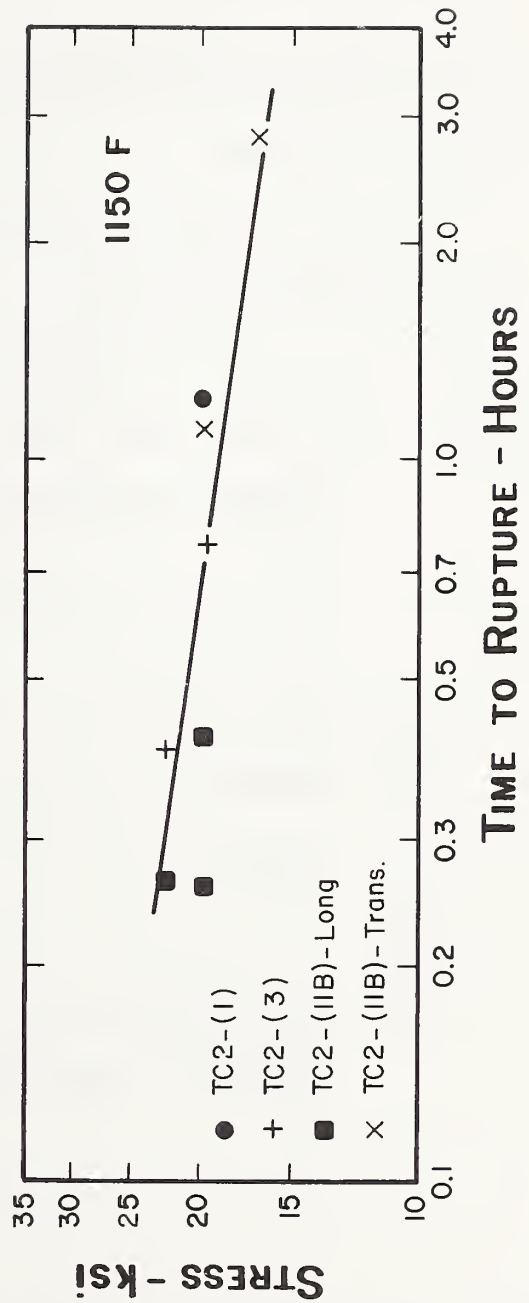


Figure 8. Elevated Temperature Yield Strength Properties of AAR M128-B Steel.





(a)

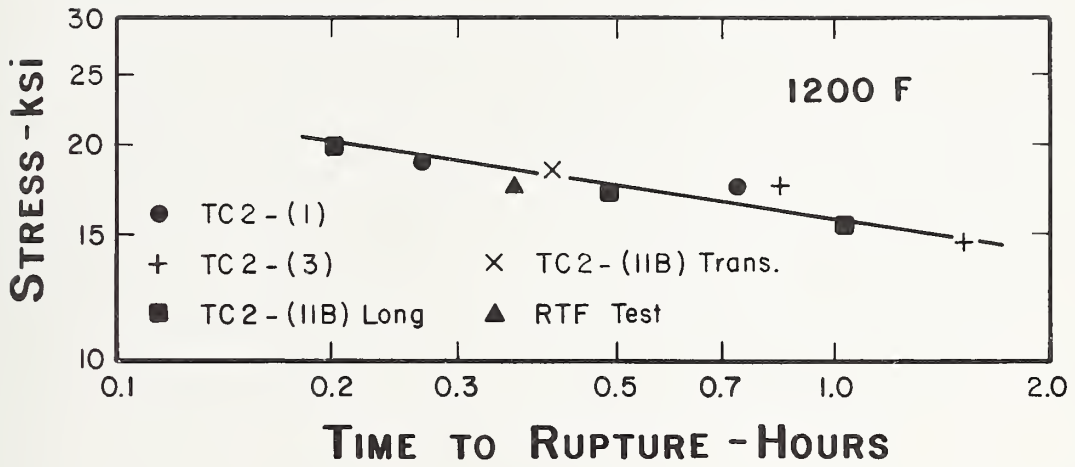


(b)

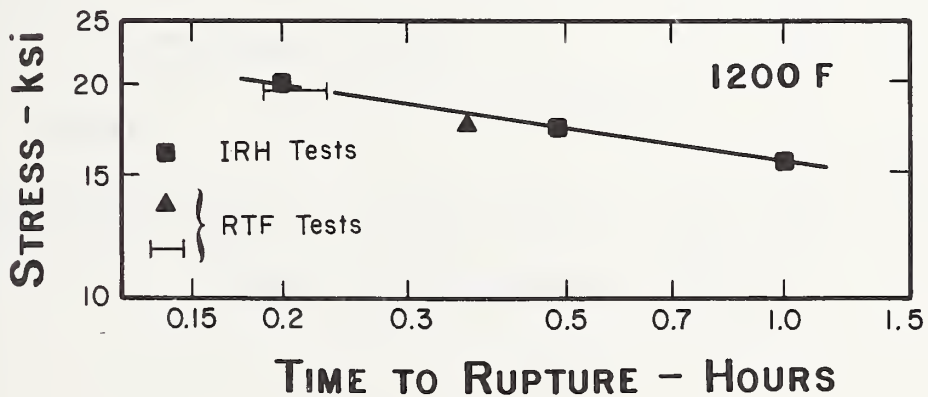
Figure 9. Stress-Rupture Data for Three Plate Samples from Tank Car RAX 202, AAR M128-B Steel.

- a. Test Temperature = 1100 F
- b. Test Temperature = 1150 F





(a)



(b)

Figure 10. Stress-Rupture Data for Three Plate Samples from Tank Car RAX 202, AAR M128-B Steel.

- a. Test Temperature = 1200 F, all specimens included.
- b. Test Temperature = 1200 F, longitudinal specimens from TC2-(11B) tested by both IRH and RTF methods.



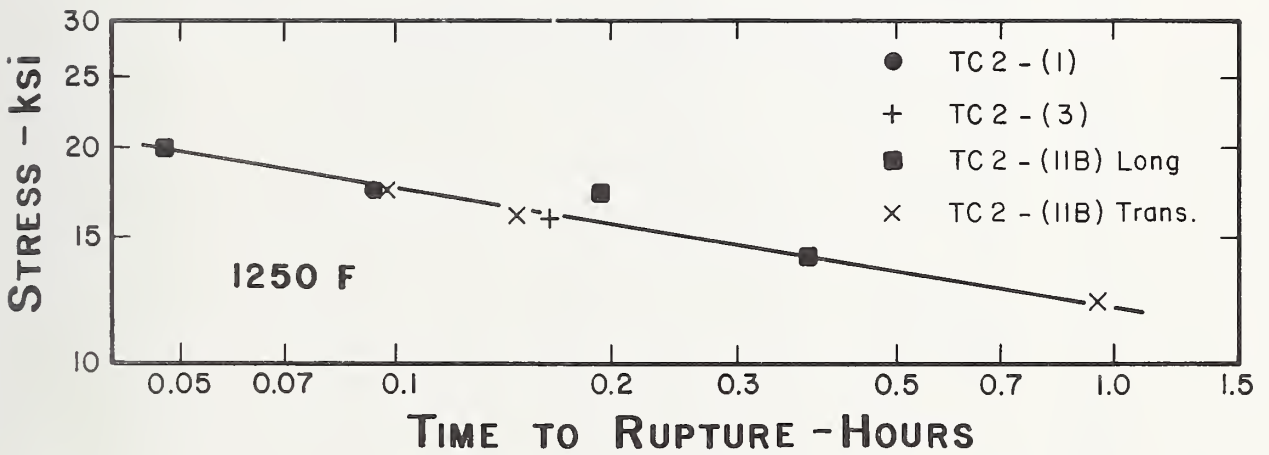


Figure 11. Stress-Ruptures Data for Three Plate Samples from Tank Car RAX 202, AAR M128-B Steel.

Test Temperature = 1250 F



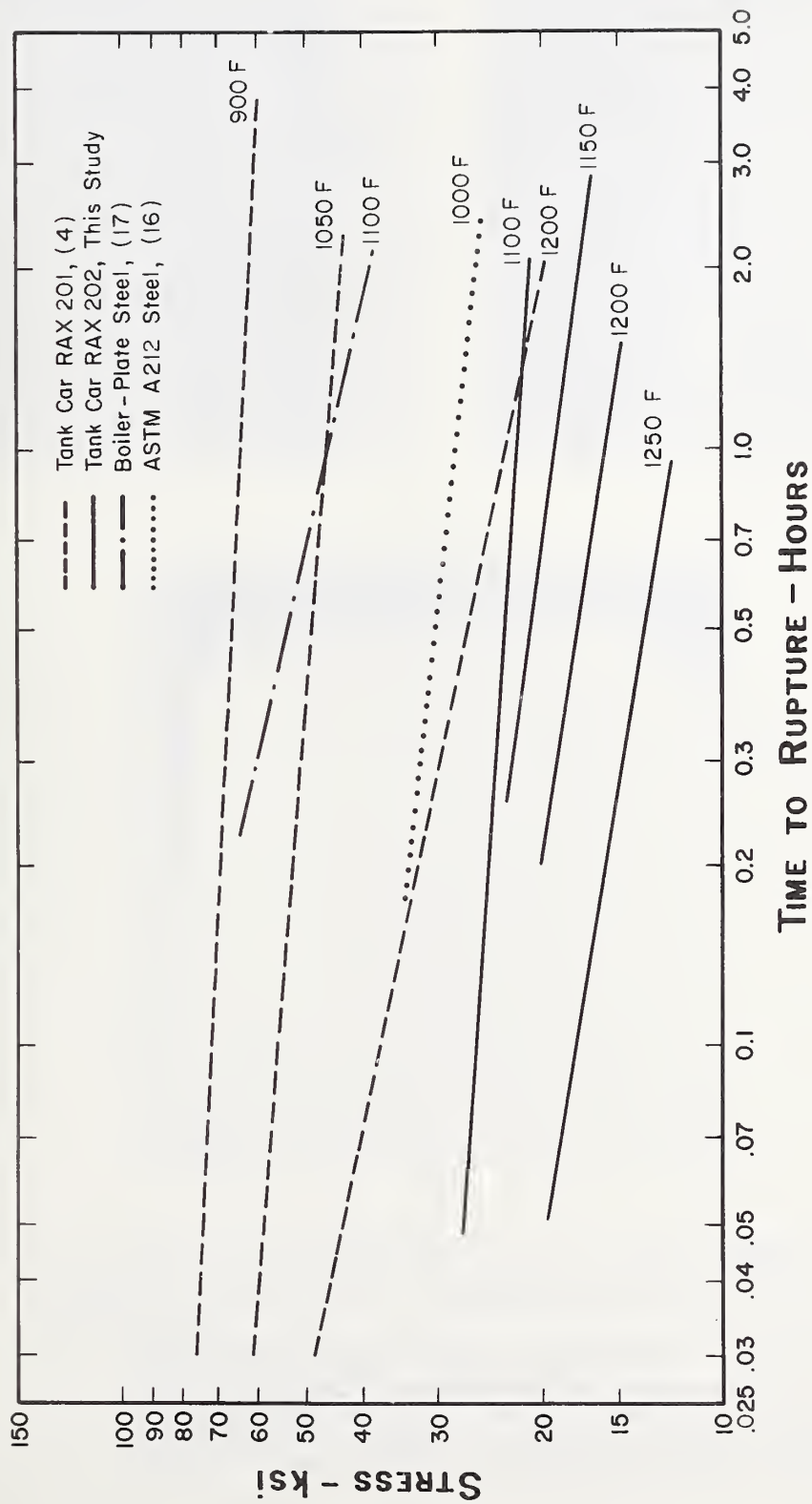


Figure 12. Stress-Rupture Data of Several Pressure Vessel Steels.

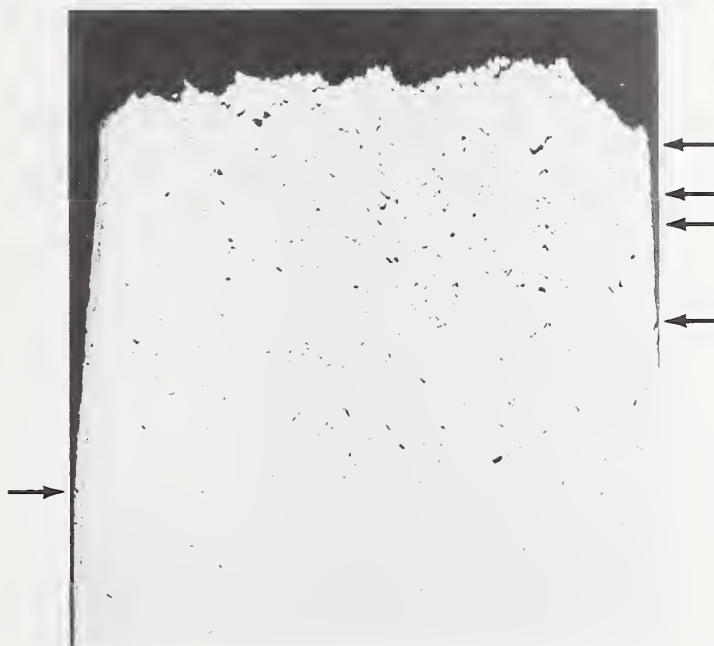




a



b



c

Figure 13. Hot Tension Test Specimen No. 21, Plate Sample TC2-(11B).  
Tested at 1100 F at a crosshead speed of 0.005/0.05 inches per minute.  
a. Photograph of exterior of specimen surface at the fracture surface. Mag. X 15  
b. SEM photograph of exterior of specimen surface at the fracture surface. Mag. X 18  
c. Photograph of fracture profile section, arrows indicate some of the secondary surface cracks. Mag. X 20





a



b



c

Figure 14. Hot Tension Test Specimen No. 38, Plate Sample TC2-(11B).  
Tested at 1200 F at a crosshead speed of 0.005/0.05 inches per minute.  
a. Photograph of exterior of specimen surface at the fracture surface. Mag. X 15  
b. SEM photograph of exterior of specimen surface at the fracture surface. Mag. X 16  
c. Photograph of fracture profile section, arrows indicate some of the secondary surface cracks. Mag. X 20



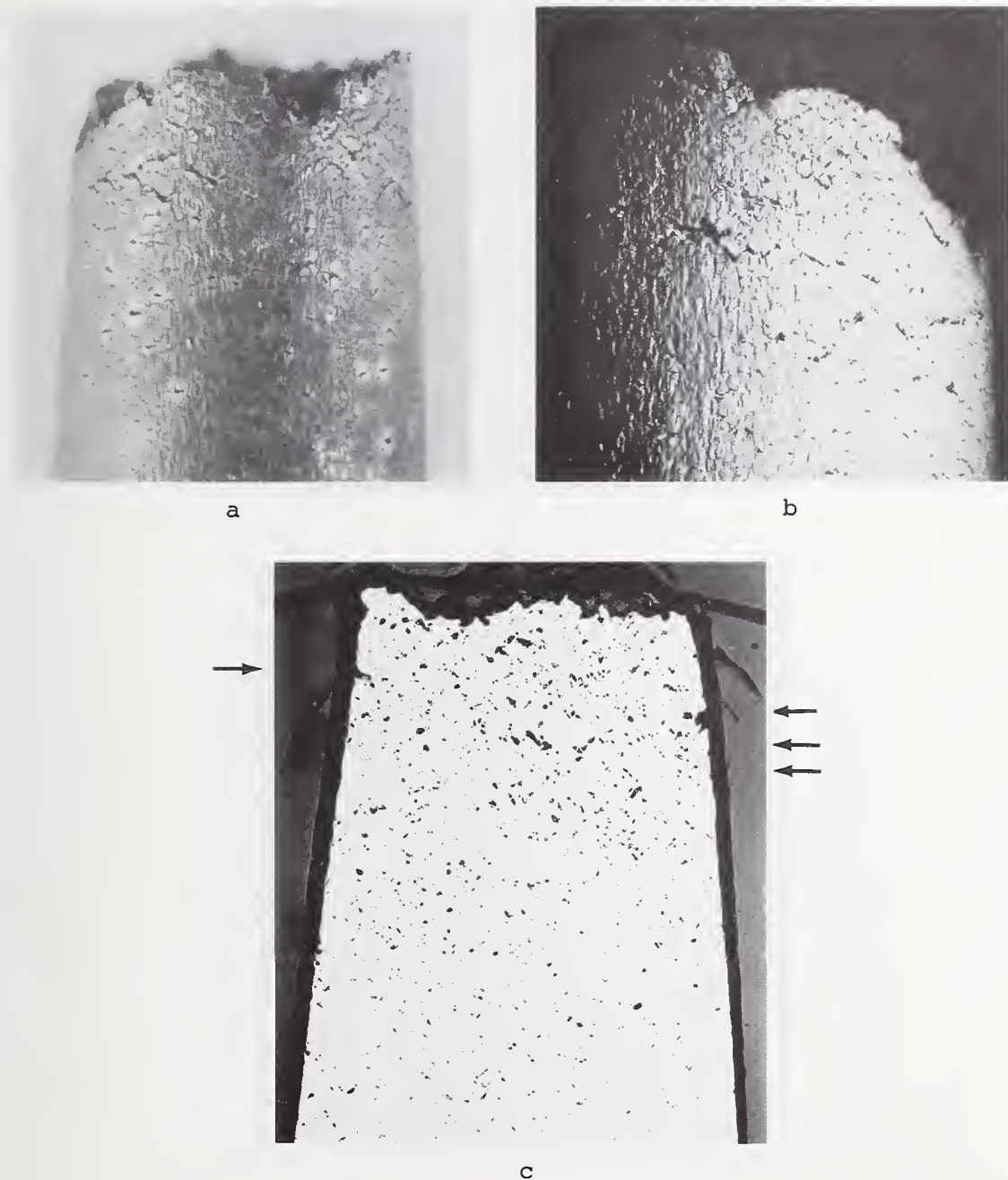
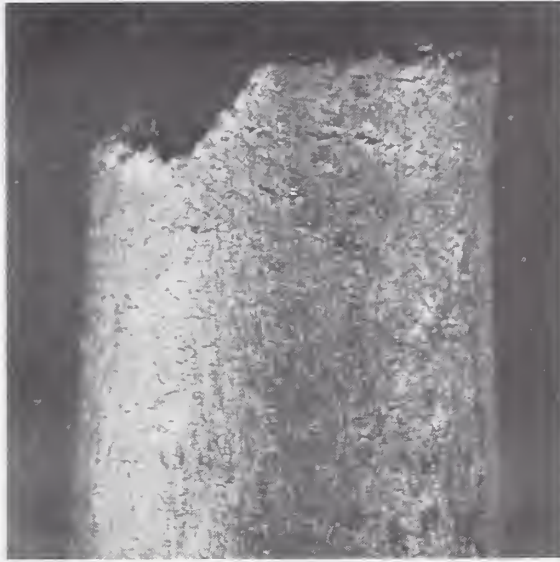
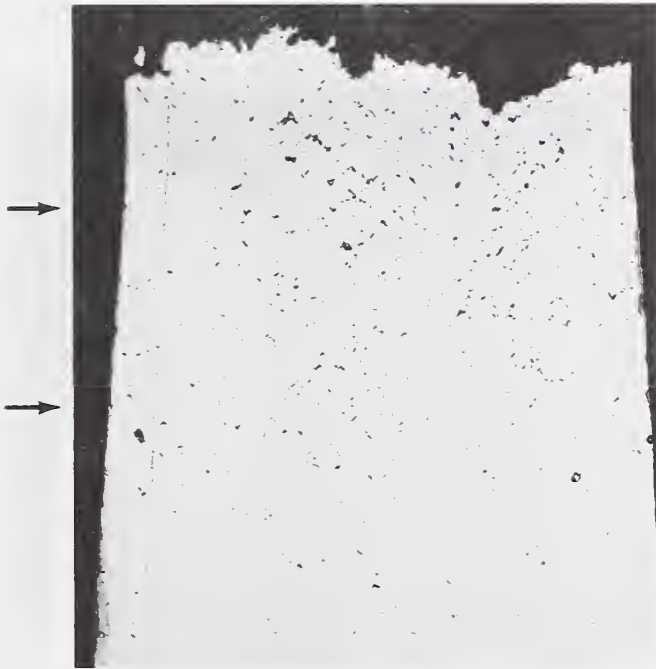


Figure 15. RTF Stress-Rupture Specimen No. 25, Plate Sample TC2-(11B).  
 Tested at 1200 F, initial stress = 19.5 ksi, time-to-rupture = 0.19/0.23 hours.  
 a. Photograph of exterior of specimen surface at the fracture surface. Mag. X 15  
 b. SEM photograph of exterior of specimen surface at the fracture surface. Mag. X 17  
 c. Photograph of fracture profile section, arrows indicate some of the secondary surface cracks. Mag. X 20





a



b

Figure 16. RTF Stress-Rupture Specimen No. 32, Plate Sample TC2-(11B).  
Tested at 1200 F, initial stress = 17.5 ksi, time-to-rupture = 0.36 hours.  
a. Photograph of exterior of specimen surface at the fracture surface. Mag. X 15  
b. Photograph of fracture profile section, arrows indicate some of the secondary surface cracks. Mag. X 20





a



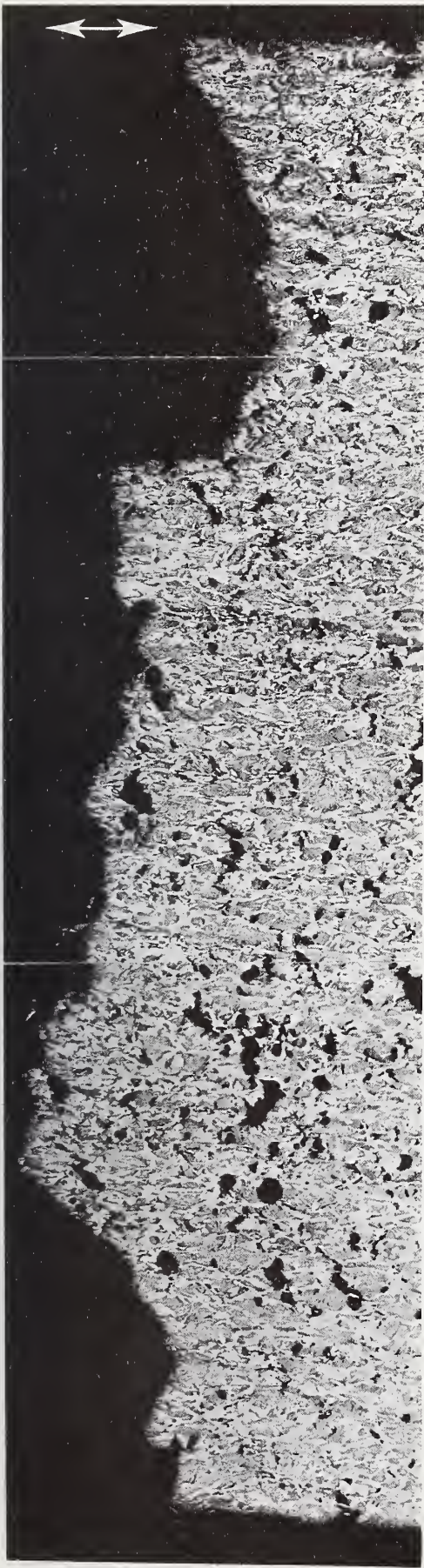
b

Figure 17. IRH Stress-Rupture Specimens.

Fracture profile sections, arrows indicate some of the secondary surface cracks.

- a. Specimen No. 42, plate sample TC2-(11B), tested at 1150F, initial stress = 22.5 ksi, time-to-rupture = 0.26 hours. Mag. X 20
- b. Specimen No. 6, plate sample TC2-(1), tested at 1200 F, initial stress = 18.9 ksi, time-to-rupture = 0.27 hours. Mag. X 20





a



b

Figure 18. Photomicrographs of Fracture Profile Sections Showing the Fracture Edge.

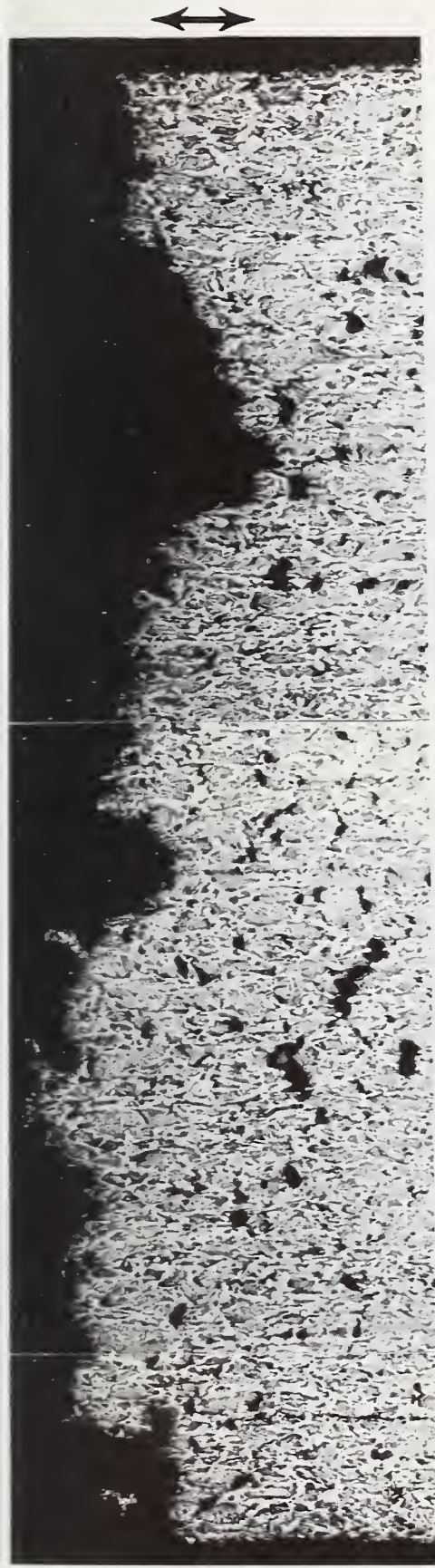
a. Hot tension test specimen No. 38, plate sample TC2-(11B). Mag. X 50

b. IRH stress-rupture specimen No. 6, plate sample TC2-(1). Mag. X 50

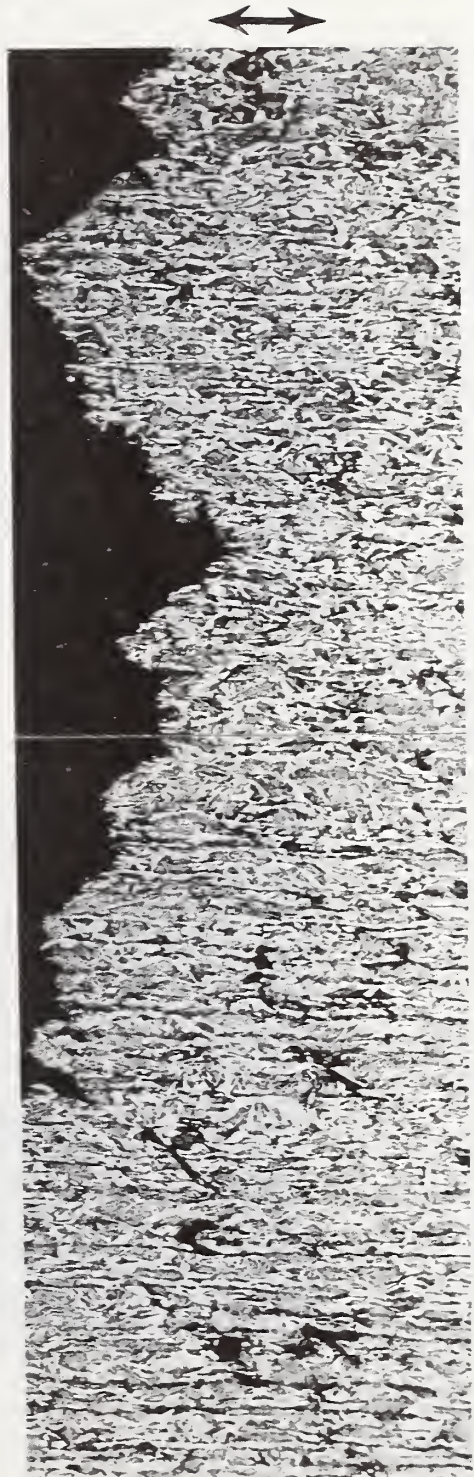
Arrows indicate direction of applied stress. Etch: 4% Picral.

Note the numerous voids beneath the fracture surfaces.





a



b

Figure 19. Photomicrographs of Fracture Profile Sections Showing the Fracture Edge.  
a. RTF stress-rupture specimen No. 32, plate sample TC2-(11B), Mag. X 50  
b. Portion of fracture profile in the region of the initial rupture of tank car RAX 202, plate sample TC2-(1). Mag. X 80  
Arrows indicate direction of applied stress, as in a., or the hoop-stress direction, as in b. Etch: 4% Picral.  
Note the numerous voids beneath the fracture surfaces.



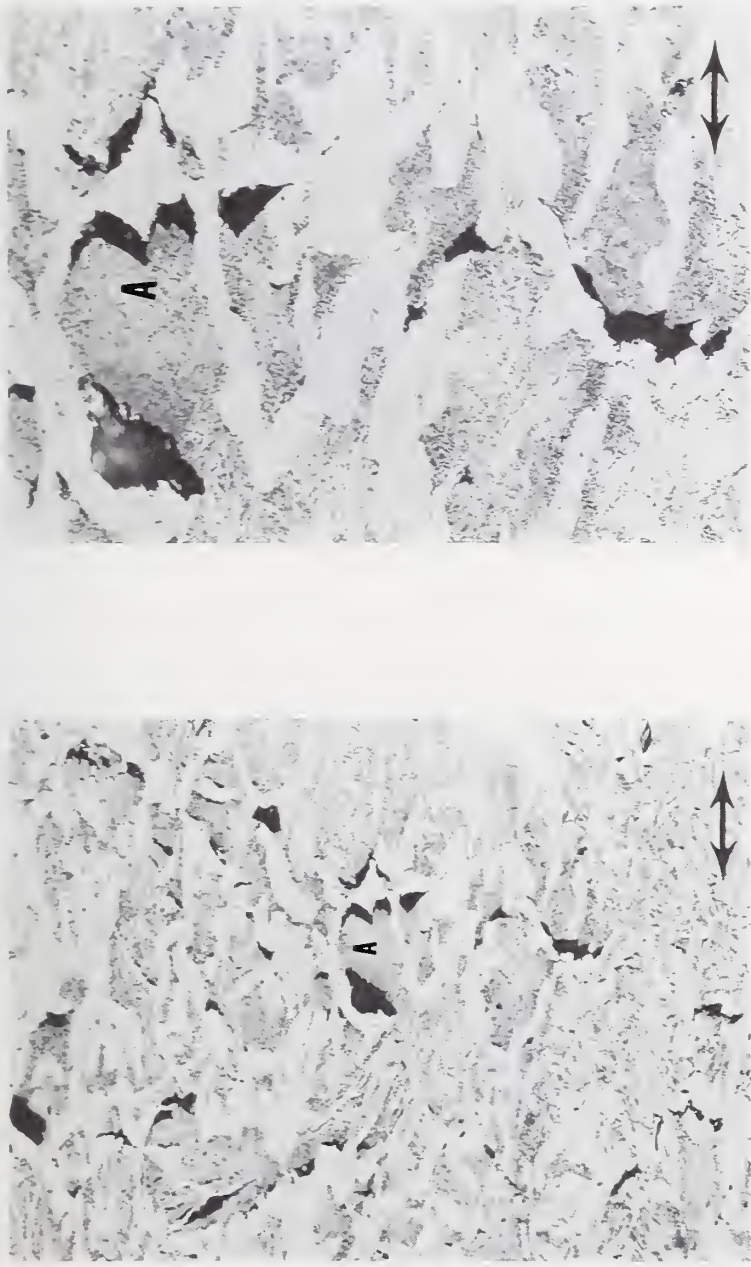


Figure 20. Photomicrographs of the Region Immediately Behind the Fracture Surface. Hot tension test specimen No. 38, plate sample TC2-(11B). The region, marked A, shows cavities forming as a result of the separation of proeutectoid grains from regions of pearlite.

- a. Mag. X 200
- b. Mag. X 500

Arrows indicate direction of applied stress. Etch: 4% Picral.





a

b

Figure 21. Photomicrographs of the Region Immediately Behind the Fracture Surface.

IRH stress-rupture specimen No. 6, plate sample TC2-(1).

a. Mag. X 200

b. Mag. X 500

Arrows indicate direction of applied stress. Etch: 4% Picral.



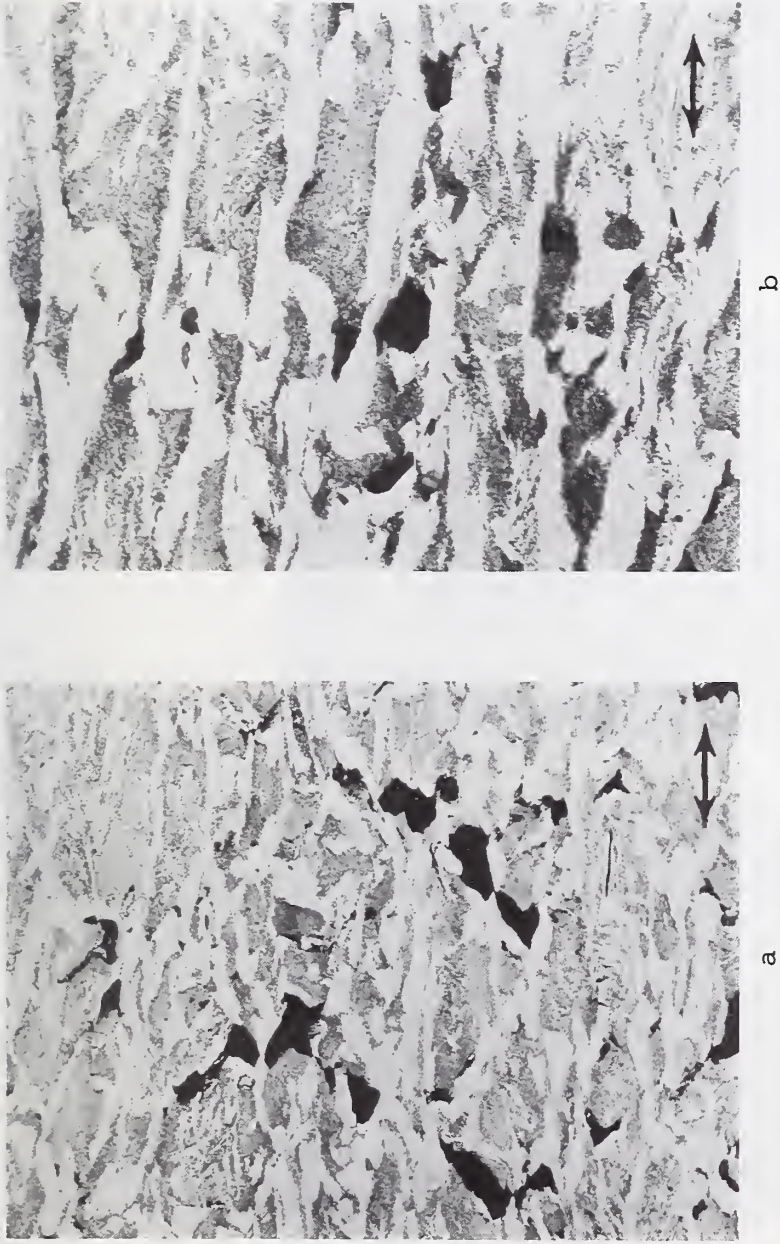


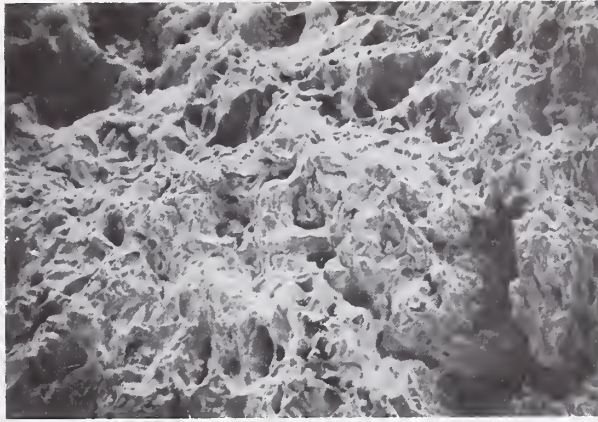
Figure 22. Photomicrographs of the Region Immediately Behind the Fracture Surface.

a. RTF stress-rupture specimen No. 32, plate sample TC2-(1). Mag. X 200

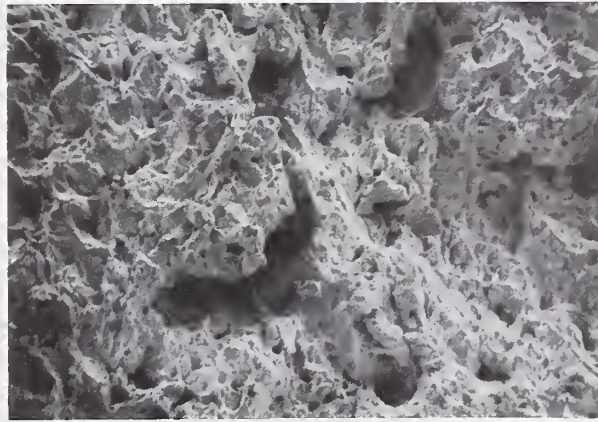
b. Region of the initial fracture of tank car RAX 202, plate sample TC2-(1). Mag. X 500

Arrows indicate direction of applied stress, as in a., or the hoop-stress direction, as in b. Etch: 4% Picral

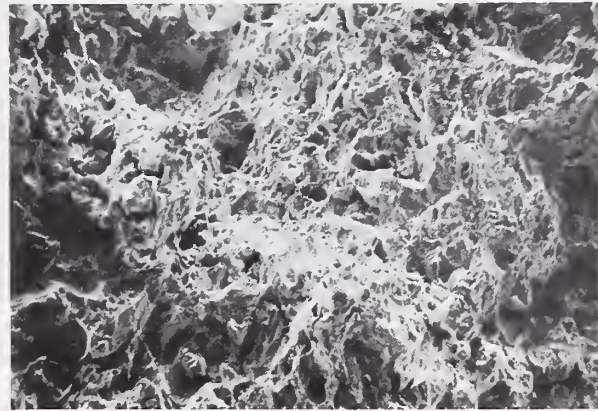




a



b



c

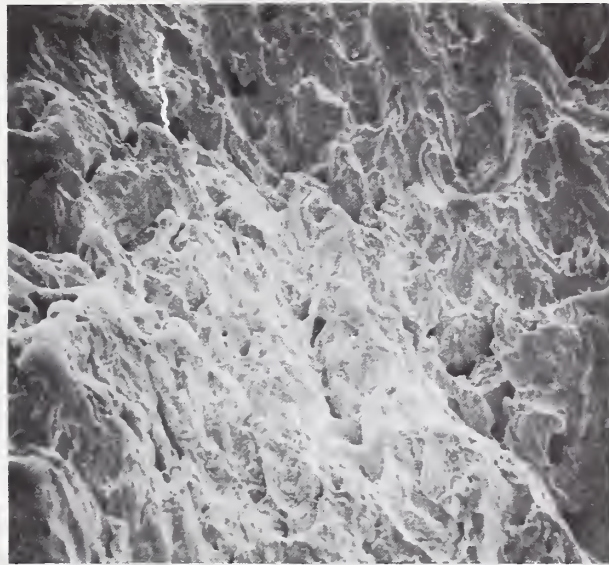
Figure 23. SEM Fractographs of Selected Fracture Surfaces, Plate Sample TC2-(11B).

- a. Hot tension test specimen No. 21, test temperature = 1100 F. Mag. X 200
- b. RTF stress-rupture specimen No. 25, test temperature = 1200 F. Mag. X 170
- c. IRH stress-rupture specimen No. 33, test temperature = 1200 F. Mag. X 180





a

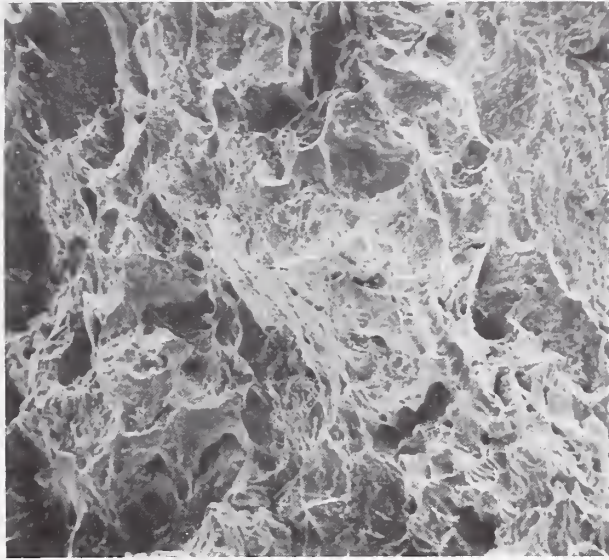


b

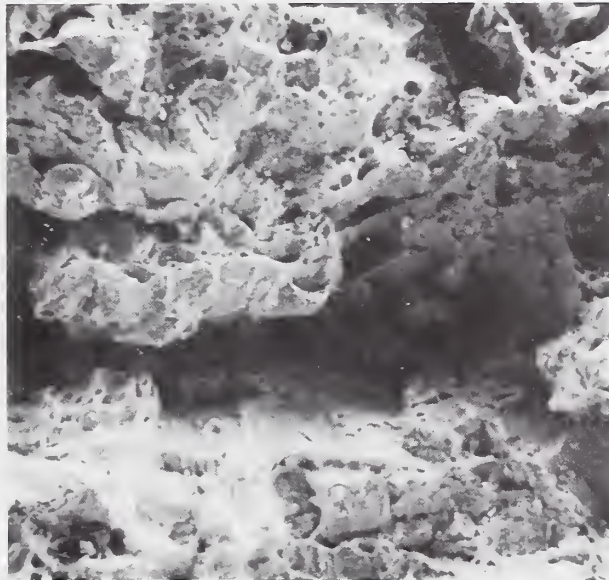
Figure 24. SEM Fractographs of Selected Fracture Surfaces, Plate Sample TC2-(11B).

- a. Hot tension test specimen No. 27, test temperature = 1150 F. Mag. X 470
- b. RTF stress-rupture specimen No. 32, test temperature = 1200 F. Mag. X 430





a



b

Figure 25. SEM Fractographs of Selected Fracture Surfaces

- a. IRH stress-rupture specimen No. 31, plate sample TC2-(11B), test temperature = 1100. F. Mag. X 430
- b. Region of initial rupture of tank car RAX 202, plate sample TC2-(1). Mag. X 525



U.S. DEPT. OF COMM. <b>BIBLIOGRAPHIC DATA SHEET</b>	1. PUBLICATION OR REPORT NO. NBSIR 75-725	2. Gov't Accession No.	3. Recipient's Accession No.
4. TITLE AND SUBTITLE Report No. 8 AMBIENT- AND ELEVATED-TEMPERATURE MECHANICAL PROPERTIES OF AAR M128-69-B STEEL PLATE SAMPLES TAKEN FROM FIRE TESTED INSULATED TANK CAR RAX 202		5. Publication Date May 1975	6. Performing Organization Code
7. AUTHOR(S) J. G. Early		8. Performing Organ. Report No. NBSIR 75-725	
9. PERFORMING ORGANIZATION NAME AND ADDRESS NATIONAL BUREAU OF STANDARDS DEPARTMENT OF COMMERCE WASHINGTON, D.C. 20234		10. Project/Task/Work Unit No. 3120413	11. Contract/Grant No.
12. Sponsoring Organization Name and Complete Address (Street, City, State, ZIP) Federal Railroad Administration Department of Transportation Washington, D. C. 20590		13. Type of Report & Period Covered Failure Analysis Report	
14. Sponsoring Agency Code		14. Sponsoring Agency Code	
15. SUPPLEMENTARY NOTES			
16. ABSTRACT (A 200-word or less factual summary of most significant information. If document includes a significant bibliography or literature survey, mention it here.) Studies were undertaken at NBS to measure the elevated-temperature mechanical properties and to determine the elevated-temperature fracture behavior of selected AAR M128-B steel plates taken from tank car RAX 202. A secondary effort was to measure the ambient-temperature mechanical properties to determine if the requirements of specification AAR M128-B-69 were satisfied. Three plate samples were selected for this study. The NBS results of check chemical analyses, hardness surveys, thickness measurements, macroscopic observations, and metallographic analyses of these plate samples had been previously reported. Results of ambient-temperature tensile tests showed that all three plate samples met the strength and ductility requirements of specification AAR M128-B-69. Results of hot-tensile tests showed a continuous decrease in strength properties and an increase in tensile ductility in the temperature range from 1100 F to 1250 F. Analysis of stress-rupture data for all three plate samples indicated that a single straight line represented the data at each test temperature. In the temperature and stress range investigated, a decrease in the initial stress of approximately 20 to 30 percent resulted in a twelvefold increase in rupture life. A comparison of the results of the metallographic analyses of hot-tensile and representative stress-rupture specimens in this study with the previously reported results on the initial rupture site in the failed shell course indicated the presence of an identical fracture mode. These results confirm the previously reported finding that the initial rupture of tank car RAX 202 was a stress-rupture crack. A comparison of hot-tensile and stress-rupture results between specimens from tank car RAX 201 and specimens from tank car RAX 202 showed substantial disagreement. The origin of the discrepancy is not apparent.			
17. KEY WORDS (List to include terms, symbols, codes, and units, if appropriate, in the first line of the summary; separated by semicolons)			
Ambient-temperature; elevated-temperature; insulated rail tank car; stress-rupture properties; tensile properties.			
18. AVAILABILITY <input type="checkbox"/> Unlimited <input checked="" type="checkbox"/> For Official Distribution. Do Not Release to NTIS <input type="checkbox"/> Order From Sup. of Doc., U.S. Government Printing Office Washington, D.C. 20402, SD Cat. No. C13 <input type="checkbox"/> Order From National Technical Information Service (NTIS) Springfield, Virginia 22151		19. SECURITY CLASS (THIS REPORT) UNCL ASSIFIED 20. SECURITY CLASS (THIS PAGE) UNCLASSIFIED	21. NO. OF PAGES 22. Price

